2011

Assessing Efficacy of Restoration Treatments in Juniper Savannas using Spatial Wavelets and Dot Grids on Aerial Photography

Erik James Apland
The University of Montana

ASSESSING EFFICACY OF RESTORATION TREATMENTS IN JUNIPER SAVANNAS USING SPATIAL WAVELETS AND DOT GRIDS WITH AERIAL PHOTOGRAPHY

By

ERIK JAMES APLAND

B. S. of Forest Management, The University of Montana, Missoula, MT, 2007

Thesis

Presented in partial fulfillment of the requirements
for the degree of

Master of Science
in Forestry

The University of Montana
Missoula, MT

June 2011

Approved by:

Sandy Ross, Associate Dean of The Graduate School
Graduate School

Dr. Carl Seielstad, Chair
Department of Forest Management

Dr. LLoyd Queen
Department of Forest Management

Dr. Anna Klene
Department of Geography

Apland, Erik James, M.S., May 2011 Forestry

Assessing Efficacy of Restoration Treatments in Juniper Savannas Using Spatial Wavelets and Dot Grids with Aerial Photography

Chairperson: Dr. Carl Seielstad

Abstract.
Across much of their diverse natural range in the Western US, species of the genus *juniperus* are expanding onto open grass and shrublands and infilling open woodland areas. In Southern Arizona's Clifton Ranger District, landscape-scale restoration treatments have been used to stall this expansion and reduce canopy-cover. This study utilizes and compares two techniques – dot-grid sampling and spatial wavelet analysis (SWA) – to estimate the efficacy of these treatments by measuring canopy-cover change pre-and post-treatment. Further, using the SWA dataset, the study explores the potential of SWA for landscape-scale ecological attribute estimation. This study found that restoration treatments significantly reduced canopy-cover with 18% and 42% mean reductions ($p < 0.001$), depending on treatment. The ability of SWA to estimate canopy-cover, and crown diameter was good in open canopy-cover (EF values up to 0.587 for canopy-cover estimation and 0.558 for crown diameter estimation), but diminished as canopy-cover increased, and systematically under-estimated as canopy-cover and crown diameter increased. Further, SWA showed that the potential for legacy tree and juniper expansion mapping was promising (68 to 79% of legacy trees correctly identified). Huge quantities of data and high technical complexity make SWA unsuitable for widespread adoption without addition of user-friendly interface, but the quantity and quality of data suggests a vast utility in future forest and rangeland research and management.

Table of Contents

Figures and Tables

Figure

Table

Introduction

Juniper Expansion and Infill

Since the beginning of the 19th century, woody plants have invaded and filled in open grasslands and savanna habitats worldwide (Archer et al. 1995). In the United States, over the range of geography inhabited by the genus *juniperus*, woody shrubs and trees of this genus have invaded previously-open sites (expansion), outcompeted their rivals on sites they historically inhabited, and infilled open woodlands, changing their character from open to closed (Archer et al. 1995, Jacobs 2008, Romme et al. 2008). Some of these changes may be attributed to management actions of the US Forest Service and other land management entities, especially a doctrine of total fire suppression and extensive and intensive grazing practices (West and Van Pelt 1987, Covington and Moore 1994). Further, fluctuations in climate or CO_2 availability over centuries may have altered the distribution, extent, and character of vegetation communities through time (Miller and Wigand 1994, Archer et al. 1995).

It is often postulated that changes in juniper vegetation systems occurred due to the virtual removal of fire from the ecosystem during the majority of the 20^{th} century (Baker and Shinnemann 2004). In this vein, research of fire history and fire ecology in pinon-juniper abounds. A 2004 literature review by Baker and Shinneman compares forty-six separate studies. This review found that the fire history and fire ecology of this ecosystem type is highly variable, and a subject of debate. Though it is sometimes accepted that juniper landscapes burn regularly at low severity (mean fire interval estimated at less than thirty-five years), this assertion over a broad area is not firmly based in science (Baker and Shinneman 2004).

The study area for my research is a portion of the Clifton Ranger District, Apache-Sitgreaves National Forest in Arizona that is dominated by juniper savanna and woodland. Analysis of fire scars on old-growth alligator juniper and pockets of ponderosa pine indicates that fires occurred on Clifton Ranger District every three to seven years on average in ponderosa pine stands and surroundings, and less frequently, every twenty to forty years in pinon-juniper associations (Clifton Ranger District 2008). These relatively frequent fires may have kept vegetation communities from converting to subsequent successional stages (Johnsen 1962, Miller and Wigand 1994).

Detrimental Effects of Juniper Habitat Change

Expansion and infill of juniper through greater survival due to decreased fire activity, site changes due to livestock grazing and vegetative succession (Johnsen 1962, Burkhart and Tisdale 1976), and possibly reduction of vegetative competition by grazing animals (Johnsen 1962) have led to an increase in canopy-cover in once open or lightly wooded areas in my study area on the Clifton Ranger District (Clifton Ranger District 2008). Although desired canopy-cover percentage ranges generally from between one and twenty percent in savanna and woodland, US Forest Service monitoring indicates actual percentage now ranges from six to thirty-six percent, and as high as sixty-two percent in some locations (Clifton Ranger District 2008). These areas of closed canopy have been linked to decreased productivity and diversity of understory species, whether the main agent of these decreases is shading or litter cover (Blackburn and Tueller 1970, Jacobs 2008, Jameson 1966). In pre-settlement times, most of the canopy-cover was comprised by large alligator juniper (*juniperus deppeana*) trees over fifty cm in diameter at the root collar (Clifton Ranger District 2008). Recent field surveys have found that now less than five percent of canopy-cover comes from these larger trees, and that the landscape has experienced widespread juniper expansion and infill (Clifton Ranger District 2008). Most canopy-cover now is provided by trees less than twelve cm in diameter, indicating a change in forest structure away from open, old-growth stands, to more closed stands of younger and/or smaller trees.

Juniper canopy-cover increase has also led to a decrease in herbaceous vegetation production. Using both aerial and ground-based photographs from previous decades, Clifton managers concluded that herbaceous production had fallen off with increasing canopy-cover. (Clifton Ranger District 2008). The conversion of open savannas and the closing of once-open woodlands have caused a reduction in quality habitat for a variety of wildlife species (Clifton Ranger District 2008).

Soil characteristics are also negatively impacted by increases in canopy-cover. In arid environments like that of the study area, increased tree biomass alters the soil water budget, potentially monopolizing soil water and leaving inter-canopy zones drier and less hospitable for plant germination (Wilcox and Davenport 1995). Less herbaceous ground cover, resulting from either decreased available sunlight, intercepted precipitation, or cover by leaf litter increases the erodibility of now-exposed soils (Jameson 1966, Blackburn and Tueller 1970, Wilcox and Davenport 1995).

Restoration Treatments

The fire management personnel of Clifton Ranger District have used mechanical thinning and extensive prescribed burns to attempt to restore landscapes to pre-settlement levels of canopy-coverage and species composition of under- and over-story plants. Mechanical thinning includes the use of heavy equipment or chainsaws to cut and pile vegetation for burning at a later time – referred to hereafter as "thin-and-burn." Thin-and-burn treatments both reduce canopy-cover outright by removing tree crowns and provide greater available fuel to promote continuous fire spread and increase intensity.

Fire is most widely used on the Clifton Ranger District because it makes possible the treatment of thousands of hectares (ha) in a short amount of time for a comparatively small amount of money (Clifton Ranger District 2008). Treatment of 10-20,000 ha costs about $200,000, with per ha costs in Mesa project area of $5 for burning and $48 for thin-and-burn and $3 and $48 respectively in the NO Bar project area (Lever 2010).

Research has found that fire tends to kill smaller juniper trees (Jameson 1962, Dwyer and Pieper 1967, Baker and Shinneman 2004) in the size class Clifton Ranger District managers would like to eradicate (Clifton Ranger District 2008). Restoration burns are carried out in near-wildfire conditions, in the early spring and late fall (Clifton Ranger District 2008). The availability of fuels to fire is high in warm, dry conditions, and fire effects are often suitably severe to top-kill juniper trees (Clifton Ranger District 2008). These weather and fuel conditions also allow for rapid and continuous fire spread, increasing the efficiency of restoration treatments.

Alligator juniper is particularly noted for its prolific re-sprouting following disturbance – including top-kill by cutting, mechanical "pushing" with heavy machinery, and fire (Tirmenstein 1999). The most vigorous re-sprouters are the smallest individuals, and this propensity tapers off and disappears with larger, older trees (Tirmenstein 1999). Given this problematic fire ecology, Clifton managers plan burns as recurrent treatments, not single events (Clifton Ranger District 2008). Reducing canopy-cover to promote fine fuel production could potentially lead to more regular fire, keeping re-sprouting individuals at bay into the future.

Scientific understanding regarding the effectiveness of thinning and fire in stalling juniper invasion and infill has diversified in the last decade (Baker 2009). Specifically, the prioritization of fire and thinning in reducing juniper canopy-cover is being challenged as a

general restoration need compared to limiting the spread of invasive plant species (Baker and Shinneman 2004, Baker 2009). Whether the traditional assumptions and restoration approaches described above are valid in the long run, or newer understanding leads to different restoration activities and goals which will displace them, management based on this traditional understanding is occurring across the West (Baker 2009). Ultimately, though one general restoration goal may not prove beneficial given the huge variety and spatial extent of juniper, burning and thinning for canopy reduction may prove effective in some specific areas where treatments have been sufficiently tailored to local environmental factors.

This study uses two techniques to examine the efficacy of restoration treatments in juniper savannas on the Clifton Ranger District, and test the validity of fire managers' observations that some landscapes, based on soil characteristics, produce more favorable fire effects than others. Further, a remote-sensing technique is implemented to characterize vegetation size and trends in expansion and legacy tree location and density.

Terrestrial Ecosystem Units

The 1987 Terrestrial Ecosystem Survey (TES) of the Apache-Sitgreaves National Forest (Laing et al. 1987) divides the forest into 123 Terrestrial Ecosystem Units (TEU) based primarily on soils and taking into account vegetation, climate, and special management concerns and other characteristics (Laing et al. 1987). These comprehensive surveys are described in a 1990 USFS Southwest Region directive (US Forest Service, 1990) as:

> *…[a] systematic analysis, classification and mapping of terrestrial ecosystems. This integrated survey is hierarchical with respect to classification levels and mapping intensities. A terrestrial ecosystem is an integrated representation of the ecological relationship between climate, soil and vegetation. Phases of terrestrial ecosystems form the mapping units of the TES.*

Through observation of prescribed fire effects, Clifton managers formulated the initial informal hypotheses regarding which of these units seemed to most produce desired fire effects, and which seemed most often to need additional thinning treatment to produce desired effects (Clifton Ranger District 2008, Lever 2008). TEU type 632 is thought by Clifton managers to possess greater water-holding capacity from its higher clay component. Theoretically, this soil type should sustain a more productive and continuous fuelbed. Fire introduced in warm, dry

conditions to these units could, in theory, achieve sufficient intensity to produce juniper mortality. Conversely, managers have observed the need for supplemental thinning in areas where fine fuels are not sufficient to carry and sustain intense fire. These areas are classified by the TES as 589 and 630. According to the TES data, these three TEU types have similar soil characteristics (classified as Vertic Argiustolls (589) and Lithic Argiustolls (630 and 632)) but TEU type 632 generally tends to occur on steeper slopes (15 to 45%) than TEU types 589 and 630 (0-15%) (Laing et al. 1987). Clifton managers began to direct the application of restoration treatments based on the differences in effects by TEU type, and documented these observations in official reports (Clifton Ranger District 2008, Lever 2008).

I have not found previous research that advocates such explicit use of specific TEU classifications to guide treatment applications for ecosystem restoration. The intent of the surveys of the Southwest Region of the Forest Service was to provide information to direct land management in multiple disciplines (US Forest Service 1990), however. Southwest Region national forests reference the utility of the TES data in planning and monitoring (such as on Arizona's Kaibab NF website: Kaibab NF 2011). Ganey and Benoit (2002) suggest the use of TES survey data to identify habitat for the endangered Mexican Spotted Owl (*Strix occidentalis lucida*) on National Forest Lands in the Southwestern US.

Multitemporal Aerial Image Analysis

Vertical aerial imagery has long been used to quantify vegetation changes on the ground at varying scales (Miller 1999). For example, vegetation changes have been tracked by using a record of historical aerial photographs in the Negrito watershed in New Mexico, adjacent to the Clifton Ranger District (Miller 1999). Miller suggested such photographs can be used to select desired historic conditions, while keeping in mind the natural variation within a system over time and space. Miller also noted the value of photographs to identify areas of increased canopy-cover. Though Miller used comparable aerial photographs to those in this study, he created polygons of cover class based on ocular estimates, and did not sample directly from the aerial photographs.

Land managers on the Clifton Ranger District are most concerned with areas of increasing canopy-cover and subsequent decreased understory productivity (Clifton Ranger District 2008). This study focuses on measuring canopy-cover change, as it can be measured

effectively with aerial photography at sub-project-level scale (Anderson et al. 1969, Clark et al. 2004). Indeed, though high spatial and spectral resolution is becoming more available (1 m spatial resolution, four-band (red-green-blue and near infrared) imagery was available in this area from 2007), such data do not exist depicting historic scenes. The identification of live trees in multi-spectral imagery with the aid of a near infrared band, then, is not an option using older scenes. Multi-spectral Landsat imagery of the study area was available for the time period of interest, but spatial resolution is too low (15 m in imagery since 1999) to be of aid in identifying individual tree canopies. Finally, aerial photography is the most practical source of remote sensing data given their widespread availability and use at the Ranger District level, where fuels planning and treatment implementation occurs.

Estimating environmental attributes using aerial imagery is generally accomplished using either a sampling scheme to manually classify a subset of the total image and its features, or using an image analysis technique to process the entire image area and identify features automatically based on a preset rule. In this study I used a technique from each of these categories, described below.

Digital Mylar

The US Forest Service Remote Sensing Application Center (RSAC) in 2004 developed a dot-grid sampling extension to operate in the ESRI ArcGIS (ESRI 2006) environment (Clark et al. 2004). This extension allows users to populate polygons in ArcGIS® with either a user-defined number of randomly spaced points, or with a grid of points spaced an equal (user-defined) distance apart. Selecting and attributing points based on the underlying imagery, the user can quickly estimate parameters (mean, total, abundance) of a feature of interest. This tool seemed a fitting choice for this project, as many forestry professionals and students of forestry have experience with this type of sampling on hard-copy photographs. Indeed this sampling method resembles the layout of common plot sampling schemes used to estimate environmental attributes such as forest fuel loading, and would likely be familiar to US Forest Service employees.

Spatial Wavelet Analysis

Spatial wavelet analysis (SWA) is a novel approach in remote sensing used to identify and characterize certain attributes in natural systems (Dale and Mah 1998), such as the trees, shrubs, or canopy gaps. Conceptually the wavelet function is similar to that of the Fourier analysis, a more traditional remote sensing tool. Where SWA differs from more traditional approaches is its lack of a "stationarity" assumption, relying instead on a moving window sequentially analyzing data (Dale and Mah 1998).

As the window moves over data space, it reports a range of agreement between its shape and the "shape" of the pixel values which underlie it in the data (Dale and Mah 1998). Different wavelet functions representing different wavelet shapes are used in a variety of contexts to best "fit" or identify objects of interest in a scene. Wavelets have be used to analyze time-series data (identifying peaks and valleys in populations), identify astronomical features (light features on a dark background), or, as in the context of this study, analyze environmental images to quantify ecological attributes such as forest gaps or vegetation cover (Bradshaw and Spies 1992, Slezak et al. 1992, Dale and Mah 1998, Strand et al. 2006). Dale and Mah (1998) provide a figure (reproduced here as Figure 1) which shows the concepts of the wavelet template, data sequence, and wavelet "fit." A more detailed description of the wavelet function's mathematical foundation, rationale, and utilities can be found in and Chui (1992) and Daubechies (1992), in addition to the above citations.

The SWA function used in this study is the "Mexican hat" wavelet, so called for its resemblance to a distinctive *sombrero* with its major central peak and surrounding circular ridge. This function is thought to match the form on a juniper crown in aerial photography (Figure 2) – round with smooth edges (Strand et al. 2006).

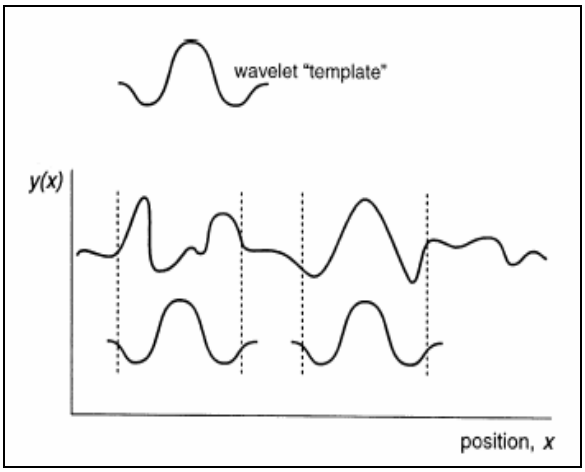

Figure 1. From Dale and Mah (1998), depicting the wavelet template and with a relatively poor fit on the left and a good fit on the right. The fit on the right would receive a positive value to denote a match with the template.

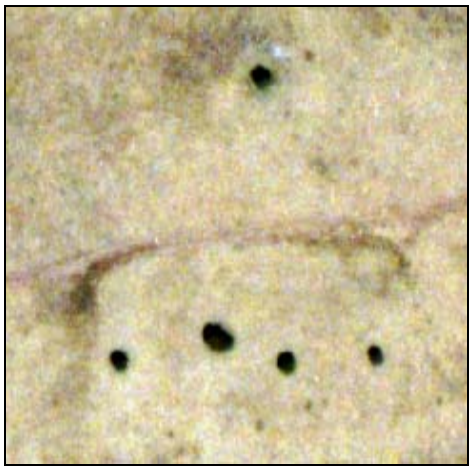

Figure 2. The typical form of a juniper crown in 0.245m resolution aerial photography – circular with smooth edges, standing at high contrast against a light, uniform background.

The wavelet algorithm is designed to search the image not just for a single template size, but for a range of user-defined sizes (Strand et al. 2006). Strand et al. (2006) describes a "range of dilation scales selected by the likely crown diameters of juniper trees (i.e. 1 to 10 m in increments of 0.1 m). . ."

Strand (2007), Strand et al. (2006 and 2008) and Garrity (2008) have shown the value of the SWA in identifying individual plants in similar ecosystems – semi-arid open woodlands and shrub steppe environments. Indeed, they have found SWA is effective in finding locations of objects and of estimating the size of these objects with reasonable accuracy and precision. In Strand et al. (2006), the SWA results from a small, open study area of juniper and sagebrush (fifteen ha, under ten percent canopy-cover) showed a five percent commission error and eight percent omission error, with sizes of identified crowns matching crown measurements in GIS with a Pearson's r value of 0.96. On a larger scale (20 60m^2 plots), Strand et al. (2007) found that commission error remained low (none recorded) but omission error rose to nineteen percent.

My study provides estimates of canopy-cover using the two methods described above, indicating areas of positive and negative change. The association between TEU type and burn effectiveness will be tested and discussed. I will implement, evaluate, and discuss the application of the Mexican hat SWA on a landscape scale. The value of SWA in identifying tree locations and sizes, characterizing forest structure, and locating legacy trees will be tested and discussed.

Finally, this study describes the strengths, shortcomings, and areas for future research regarding spatial wavelet analysis in landscape-scale ecological questions.

Methods

Overview

I employed two techniques – RSAC's Digital Mylar extension and an SWA algorithm – to analyze forest attributes in the study area in the years 2000 and 2008, depicting the same area pre- and post-restoration treatment. Both techniques used color aerial photography covering 14,700 ha as the data for analysis.

Study Area

This study focuses on restoration treatment areas on the Clifton Ranger District, Apache-Sitgreaves National Forest (NF). The Mesa and NO Bar project areas are in the center of the district, which is the southernmost of the national forest. The district is located in the vicinity of the towns of Safford and Clifton, AZ, about 160 km east of Tucson, against the New Mexico border to the east (Figures 3a and b). Elevation ranges on the district from 1100 to 2800 m ASL over the 220,000 ha of the district.

Clifton Ranger District is largely of a remote character, with few roads and steep topography (Apache-Sitgreaves NF 2011). The district hosts a variety of vegetation communities: riparian broadleaf systems, arid grasslands, chaparral, and forests and woodlands of pinon-juniper, ponderosa pine, and higher elevation fir and spruce (US Forest Service website 2011). The Mesa and NO Bar project areas include mesa-top open juniper savannas, and pinon-juniper woodlands surrounding these mesas (Clifton Ranger District 2008).

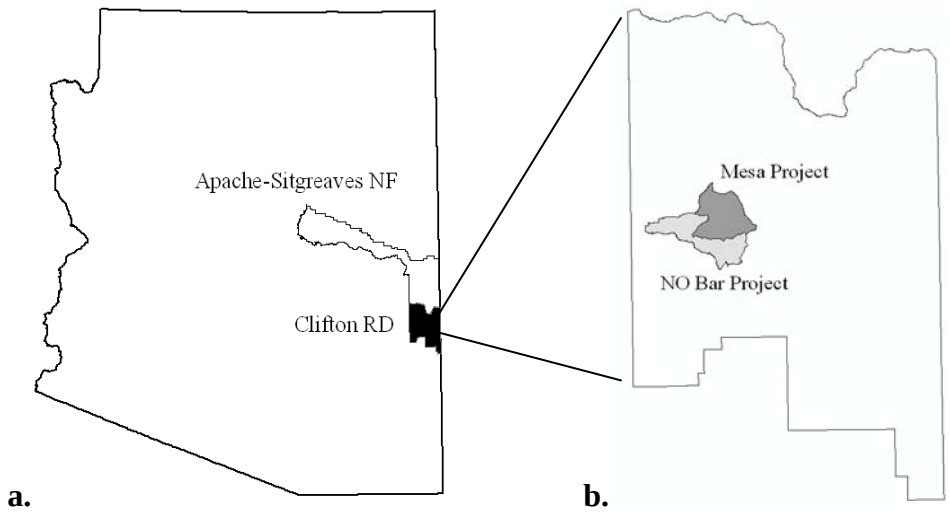

Figures 3a and b. Clifton Ranger District of the Apache-Sitgreaves NF, in southern Arizona (a) and the Mesa and NO Bar project areas within the District (b).

Aerial Photograph Digitization and Preparation

Nine-by-nice inch, color aerial photographic prints covering the project areas (scanned at 1840 dpi or 14µm) provided the data for digital analysis and interpretation. The photographs have a scale of 1:15,840, and the digital images a spatial resolution of 0.245 m. These photographs, provided by the Clifton Ranger District, were captured in two flights (in 2000 and 2008) and thus the equipment used and other details of the flights differed from each other. Regardless, the contracting company for each flight provided documentation describing the camera and lens used, including geometry parameters, such as focal length, point of autocollination, and fiducial mark location, among others (Appendices F and G).

I used the Autosync Workstation in ERDAS Imagine® 9.3 (ERDAS 2008) to ortho-rectify each scanned aerial image. Besides the individual scanned images, the ortho-rectification process requires a reference image to register each image, and a digital elevation model (DEM) and geometric model to rectify images in three dimensions. To fulfill these requirements I used 1 m resolution, National Agriculture Imagery Program (NAIP) wall-to-wall ortho-photos acquired in 2007 as a reference image; a 10 m resolution DEM (US Geological Survey 2011); and documentation of camera geometry provided with the photographic prints. I matched the coordinates of eight fiducial marks from the original film documentation with the coordinates of the center of each of the eight fiducial marks in the raster image of each photograph using Ground Control Points (GCPs). I scattered additional GCPs (four to six per image) throughout

the scenes to cover the range of variation in elevation and viewing angle in each image. I examined the resulting individual ortho-rectified images visually to detect and eliminate, through reprocessing, any obvious deviations from the reference image.

Using a default nearest-to-nadir mosaic algorithm in ERDAS Imagine®, I stitched all individual images into mosaics, and used the color balancing function to correct for changes in illumination between scenes. I examined each seamline visually to ensure areas of the images were not duplicated or left out. Three mosaic blocks were created for 2000 and 2008, with file sizes of around six gigabytes (GB) per block. Root mean square error values for these mosaics ranged between 2 and 3 m, or 8 to 12 pixels. One mosaic scene of the entire project area was also created for each time period, with a file size of about thirteen GB. These two mosaics represent 30 individual aerial photographs of approximately one GB each. Deleting the 30% sidelap and 60% percent endlap characteristic of aerial photography in each image accounted for this large reduction in file size.

Digital Mylar Analysis

Overview

I quantified canopy-cover change systematically using a dot-grid sampling approach on the imagery described above acquired in 2000 and 2008 for the Mesa and NO Bar project areas. Both areas comprise 3900 ha each, accounting for seven percent of the total restoration treatment area on Clifton Ranger District.

Canopy-Cover Estimation

Using ArcGIS®, 64 TEU polygons were overlaid upon treatment-type polygons and clipped to treatment areas for analysis. When TEUs were classified by treatment, 385 random points were populated inside each TEU using the USFS Remote Sensing Applications Center Digital Mylar extension to ArcGIS® (Figure 4). I selected a sample size of 385 points per polygon to develop estimates with 95% confidence with margins of error of about 1%. I used identical sample sizes for each polygon regardless of its spatial extent after determining the areas delineated displayed relatively uniform cover. I examined each point and tallied each as either “on canopy” or “off canopy.” Shadowing often obscured complete tree crowns, especially on slopes. In these cases, I assumed the crown was symmetrical. I did not count points that overlay

indistinct “vegetation-like” features as canopy hits when these features cast no shadow, did not display the typical round tree form common throughout the area, and were a different shade of green than tree crowns. I compiled the resulting canopy-cover estimates – “on canopy” points divided by 385 points – resulting canopy-cover estimates were then compiled by TEU type and treatment, providing canopy-cover and change estimates over the Mesa and NO Bar project areas. Canopy-cover estimates were tabulated and grouped (Appendices A through C) by TEU type and treatment in Microsoft Excel® 2003 (Microsoft 2003).

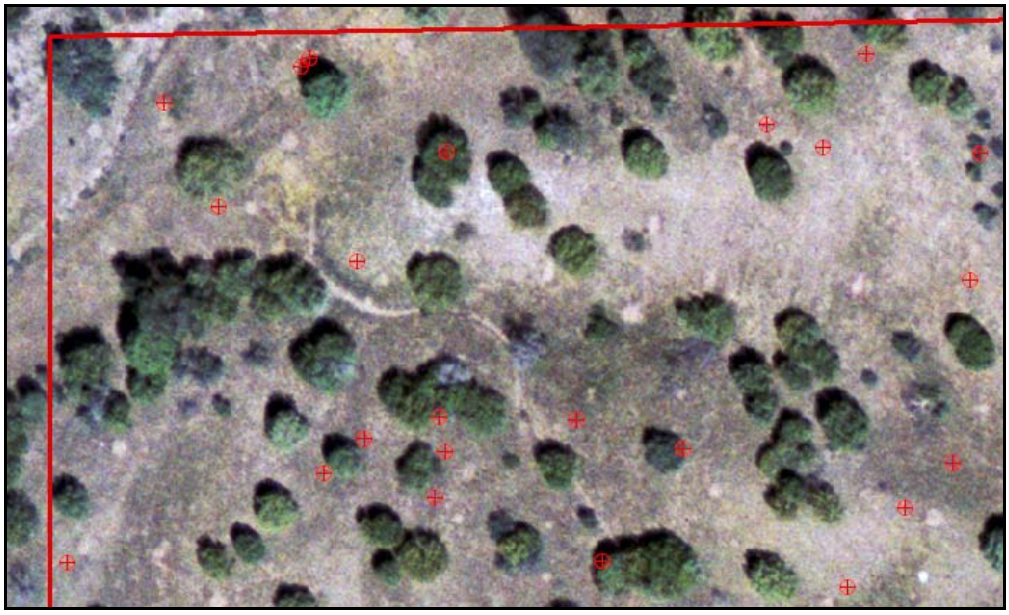

Figure 4. A section of a TEU polygon showing sample points generated using Digital Mylar.

In order to compare like polygons, I also categorized TEU polygons by topographic type. The topographic types I used were “mesa top,” where the entire polygon was situated on the top of a mesa, “draw,” where the entire polygon was situated in a draw, and “mixed,” where the polygon included both mesa tops and draws.

Finally, I investigated the proportion of TEU polygons by treatment type that had post-treatment canopy-cover which matched an average target value of under 15% canopy-cover I set based on my examination of Clifton Ranger District restoration treatment plans (Clifton Ranger District 2008, Lever 2008).

Spatial Wavelet Analysis

Overview

I also implemented a wavelet analysis developed by Dr. David Hann and furnished by Dr. Alistair Smith of the University of Idaho. This algorithm, run on The MathWorks MATLAB® 7.9 (The Mathworks 2009) programming platform, was used by Falkowski et al. (2006) and Garrity et al. (2008) and similar to the algorithm used by Strand (2007) and Strand et al. (2006, 2008). Similar to an image classification exercise, SWA data represents a census method, not a sampling method like Digital Mylar.

Data Preparation

I found through repeated trial that in using large subset areas of mosaic images, the maximum memory capabilities of text editors and the MATLAB® software were exhausted. Subsetting images into areas small enough to process at the photographs' original spatial resolution was a prohibitively time consuming process. I therefore resampled the 2000 and 2008 aerial imagery from their original 0.245 m spatial resolution to 1 m spatial resolution, using a cubic convolution resampling method in ERDAS Imagine®. I selected this method, which applies a cubic function to calculate pixel values in output images, to maintain a degree of integrity for small features in the imagery, which in nearest neighbor resampling could become indistinct or disappear entirely. Using these 1 m resolution images, I used the same mosaic process as above, selecting only the red band for mosaics, and using the color balancing algorithm in ERDAS Imagine® to correct for differences in illumination between aerial images. I selected the red band because it appeared to provide the greatest contrast between surrounding pixel values and canopy pixel values, when compared to the green and blue bands. The resultant diminution of file size allowed for the processing of image subsets of around 5M pixels each, covering an area of about 500 ha per tile.

Strand et al. (2008) used imagery at 1 m resolution, in one case resampling resolution from higher resolution to match the 1 m resolution of earlier imagery. This lower resolution resulted in a diminished ability to identify objects of about 1 m in size or smaller. In the Strand et al. (2008) study focusing on shrub cover, this inability to identify small objects proved problematic, as many shrubs were undetectable to the SWA algorithm. I considered this inevitable consequence of image resampling, but concluded that:

1. In many cases these objects were not distinguishable as trees even to the eye at 0.245 m resolution as trees (versus shrubs or other patches of vegetation), and
2. The growth of smaller juniper trees from 2000 to 2008 into trees large enough to appear distinct in 1 m resolution imagery is a measure of juniper expansion.

I subset the 2000 and 2008 1 m resolution mosaics into thirty-three tiles for each year and prepared the image area representing each of the TEU polygons areas for wavelet analysis. I created the thirty-three rectangular tiles by first dividing a shapefile in ArcGIS® 9.2 that represented the area of overlap between the two years' mosaics. I buffered each of these shapefiles by 5 m to account for those tree crowns which might fall on the boundary of the tiles and ensure the entire area was covered.

I used the tiles as templates to create area of interest (.aoi) files in Imagine, and subset the 2000 and 2008 mosaics using these .aoi files.

The final step of data preparation before files were process-ready was to convert each subset red-band image to an ASCII file format (a text file comprising a list of pixel values) for use by the wavelet transform algorithm. To perform this conversion I used the "Raster to ASCII" converter in ArcToolbox® (ESRI 2006). I removed the header from each ASCII file, transferring the left edge and top edge Universal Transverse Mercator (UTM) coordinates to a spreadsheet for later use.

SWA Algorithm Operation

The wavelet transform algorithm I used loads each ASCII image file, convolves the image using a kernel size specified by the user, and propagates a user-defined wavelet transform over the image space. The wavelet transform identifies low (dark) pixel values and finds a wavelet of matching size to fit this anomaly. The user-defined threshold value sets the threshold for the minimum amount of departure from background pixel values that the wavelet will consider an anomaly. Wavelet size and range describe the size of the initial wavelet, and the range of waves which can propagate and fit low (dark) pixel value anomalies.

Having fit a wavelet over an area of low pixel values, the wavelet algorithm records the size and location of this anomaly, drawing a circle which bounds the wavelet fit "tree."

I altered the wavelet code for two purposes – to process images in a batch, and to create output shapefiles for further manipulation and analysis in ArcGIS®. The batch process changes allow the user to load images, analyze them, and create output files sequentially based on a linear naming scheme (i.e. “2008_Tile_01”). This alteration made it possible to analyze the entire set of imagery numerous times with different threshold settings, having the computer process the files and create output in separate folders sequentially without continuous user input.

Altering the code to create ArcGIS® shapefiles as output allowed me to easily view SWA results and streamline analysis and accuracy assessment. Each tile’s shapefile was comprised of individual points with Northing, Easting, and radius information recorded as attributes for each point. Northing and Easting values were appended to the image in MATLAB to describe each identified point’s spatial location using the list of left and top UTM coordinates mentioned above. Each tile represented a large number of records – around 25,000 identified points with associated attributes.

Following recommendations in Strand et al. (2006) I chose a dilation scale of one pixel to twelve pixels, moving in steps of 0.1 pixels (after the image resampling described above, one pixel was equivalent to 1 m). The dilation scale represents the range of possible radii of tree crowns on the landscape. I set my initial wavelet size to 6 m, and chose two thresholds (30 and 70), intending one to have a high omission error and low commission error (70), and the other to have a low omission error and high commission error (30). These thresholds represent the minimum difference in pixel value required for SWA recognition of features. The enormous spatial extent and variability of the imagery made it difficult and time-consuming to choose one best threshold through empirical trial. Through this trial-and-error period, characteristics of SWA performance became evident.

Canopy-Cover Estimation

In order to produce estimates of canopy-cover, I buffered each tree center point, in ArcGIS®, by the attribute field “radius.” I then dissolved these circles of various sizes together, to eliminate overlapping canopy areas. Finally, dividing the total area of dissolved canopy-cover by the area of the TEU polygon provided a percent-cover estimate (Appendices D and E).

Accuracy Assessment

Different statistics must be used to assess the accuracy of a census than would be used in estimating the quality of a sampling method, as a census does not estimate a population parameter but instead provides an estimate for every constituent of the population. Similar to the classification of a large image, SWA presented the problem of a substantial amount of data with no automated way to assess its accuracy. An error matrix is often used to evaluate the accuracy of a sample of classified pixels to those in the original image (Jensen 1996). For these data, however, I wanted to measure the accuracy of SWA in determining crown diameter, in locating features, and in recognizing the difference between other dark features and tree crowns. Formally, I sought to estimate model efficiency and errors, along with both commission error (identification of nonexistent tree crowns) and omission error (failing to identify tree crowns).

To estimate commission error and SWA crown diameter accuracy, I selected a random sample of 146 SWA-indentified tree crowns (from the 2008 70-threshold SWA run, which I selected using a random number table). I divided these tree crowns into cover classes representing the quality of the canopy-cover immediately surrounding them: open (the crown is completely distinct from other crowns and from its background), mixed (the crown is impinged upon by other tree crowns or features in the image), and closed (the tree crown is indistinguishable from its background or other trees). These 146 points divided roughly into thirds based on this categorization: 41 in the open, 52 in the mixed, 51 in the closed category. Each class showed a small number of identified tree crowns which did not exist in the imagery. Therefore the final sample sizes were 38, 51, and 46, respectively. In GIS I measured the tree (if indeed there was one) that underlay each point, and compared this with the radius recorded by the SWA algorithm.

To estimate omission error rate I implemented a plot-sampling approach, using 10 randomly-placed 20 m radius circular plots for each SWA run and threshold setting (e.g. Year 2000, Threshold 70) in GIS. This sample size and plot area was chosen to include 140 trees per plot, matching the sample size described above. I excluded trees visible in GIS with a diameter smaller than 2m, as these small crowns are too small for SWA to reliably detect.

I used statistics measuring model efficiency (EF), mean absolute error (MAE), and mean bias error (MBE), comparing canopy-cover estimates using Digital Mylar and SWA, and SWA-

identified tree crown diameters with their GIS-measured diameters. I chose these statistics because I wanted to estimate how closely SWA results matched a one-to-one relationship with Digital Mylar results and GIS-measurements. EF, MAE, and MBE are calculated using the residuals of estimates vs. "truth" data, in this case SWA estimates of canopy-cover vs. Digital Mylar estimates and GIS-measured crown diameters. The resulting statistics provide measures of the overall value of a model (EF), the average error in model estimates (MAE) and the average bias in model estimates (MBE) (Toney and Reeves 2009). EF statistics occupy a range between -1 and +1. Negative values indicate poor model efficiency, with zero representing a model's equivalency with a simple mean of the data. Positive values indicate good model fit, with a value of one indicating perfect agreement between a model and reality (Toney and Reeves 2009). Pearson's r-values with corresponding significance levels also give a measure of model fit, though without taking bias into account, and are provided for comparison with MAE, MBE and EF.

A preliminary look at wavelet-produced shapefiles demonstrated that the algorithm tended to face difficulty in identifying tree crowns in more closed-canopy areas. Similarly, Strand et al. (2008) noted that, "In the canopy-cover range of 25-55%, SWA is biased towards underestimating foliar cover and above 55% cover the method is unreliable for analysis of aerial photography." Bearing in mind this caveat, I separated model efficiency statistics by canopy cover classes.

Results

Canopy-Cover Estimation

Estimates of canopy-cover derived from Digital Mylar dot grid sampling showed significant differences between three treatment types and levels of change characteristic of each treatment type, but no significant difference between TEU types matching my hypothesis that TEU type 632 would show greater change compared to types 589 and 630. I used SPSS Statistics® 19 (SPSS 2010) for statistical analysis and to produce figures. All change percentages were calculated as relative changes, not actual additions or subtractions (e.g. a decrease from 10% canopy-cover to 9% canopy-cover would be a 10% decrease, not a 1% decrease). Using

relative canopy-cover changes makes it possible to compare effects of treatment regardless of actual canopy-cover values.

Table 1 shows all estimates of canopy cover in 2000 and 2008. I will discuss the comparison of Digital Mylar and SWA estimates below.

There was some variability in change due to burning and thin-and-burn treatments, with ranges from no change to a -24% reduction in the burn treatment, and -21% to -69% in thin-and-burn polygons. Total change across both the NO Bar and Mesa project areas (Table 2) was -17% and -40% for burn and burn and thin, respectively. Burn and thin-and-burn treatment results were both highly significant ($p < 0.001$).

Table 1. Pre- and post-treatment canopy-cover (CC, in percent) estimates with standard errors for Digital Mylar and SWA techniques.

Digital	Treatment	n	2000 CC	S.E.	2008 CC	S.E.
Mylar	Untreated	2695	28.20	0.009	30.39	0.009
	Burn	19635	18.53	0.003	15.49	0.003
	Thin & Burn	3080	19.84	0.007	11.98	0.006
SWA 30	Untreated	7	24.94	3.250	23.03	3.546
	Burn	49	14.90	1.200	12.86	1.110
	Thin & Burn	8	16.13	1.436	10.98	1.422
SWA 70	Untreated	7	24.20	3.782	22.14	3.701
	Burn	49	13.90	1.204	11.41	1.130
	Thin & Burn	8	15.28	1.508	9.17	1.472

Table 2. Total change in all polygons for both project areas from 2000 to 2008 using both Digital Mylar and SWA techniques.

Digital	Treatment	n	Change	S.E.	Sig.
Mylar	Untreated	2695	7.97	3.24	$p = 0.15$
	Burn	19635	-17.73	2.37	$p < 0.001$
	Thin & Burn	3080	-41.74	5.59	$p < 0.001$
SWA 30	Untreated	7	-8.15	5.7	$p = 0.203$
	Burn	49	-13.61	2.22	$p < 0.0001$
	Thin & Burn	8	-33.02	4.41	$p < 0.0001$
SWA 70	Untreated	7	-9.02	2.3	$p = 0.08$
	Burn	49	-20.16	2.09	$p < 0.0001$
	Thin & Burn	8	-42.27	5.3	$p < 0.0001$

Change estimates for untreated polygons showed greater variability, however. Estimates ranged from -5% to +18%. The mean change for all seven polygons was +7%, but this result was not significant ($p = 0.15$).

To investigate differences in canopy-cover reduction by treatment in similar topographic types, I divided polygons into topographic class. Table 3 summarizes the results of this analysis, showing that the greatest reductions occurred on mesa tops. Testing change means within topographic types and between burn and thin-and-burn (with an independent samples t-test) showed that thin-and-burn canopy-cover reductions were not statistically greater ($p = 0.07$ for mesa tops, and $p = 0.06$ for mixed topography).

Table 3. Canopy-cover reduction by treatment and topographic type. There were no thin-and burn treatments in draws.

Burn Polygons				
Topographic Type	**Change %**	**n**	**S.E.**	**Sig.**
Mesa Top	-23.50	13	5.92	$p = 0.004$
Draw	-7.85	11	2.20	$p = 0.009$
Mixed	-19.08	25	3.09	$p < 0.001$
Thin & Burn Polygons				
Mesa Top	-46.80	4	9.46	$p = 0.013$
Mixed	-36.67	4	6.24	$p = 0.020$

When comparing Digital Mylar post-treatment (2008) canopy-cover estimates with the target canopy-cover of under 15% for treated TEU polygons, I found that thin-and-burn treatments also more reliably reduced canopy-cover to within the target range. Of eight thin-and-burn polygons, five (63%) had post-treatment canopy-cover of 15% or less, while two polygons (25%) were not reduced to within the target range, and one polygon (13%) already had canopy-cover under 15%. Conversely, among the forty-nine burn polygons, twelve (24%) reached target canopy-cover, twelve were already in the target range, and twenty-five (51%) showed post-treatment canopy-cover greater than 15%.

TEU Types and Fire Effects

There was no evidence from Digital Mylar estimates to suggest significant differences between burn effectiveness based on TEU types. Those polygons which I anticipated to show greater fire effects (TEU type 632) did not have statistically different change estimates ($p = 0.910$) than did other polygons: -13% canopy-cover reduction for 632 vs. -14% canopy-mean reduction for burned polygons of TEU types other than 589, 630 and 632. Further, TEU types which were postulated to require thinning in addition to burning showed significantly greater change than the theoretically fire-amenable TEU types: A mean reduction of -29% for TEU types 630 and 589, compared to the -13% reduction in canopy-cover in TEU type 632 ($p = 0.03$). These findings are summarized in Figure 5.

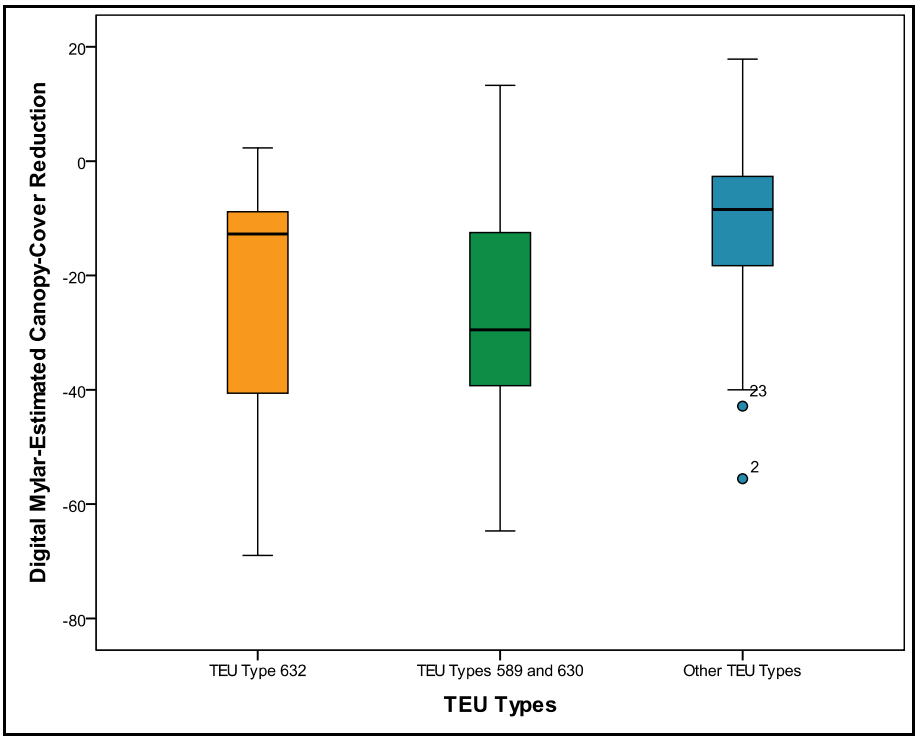

Figure 5. Means and data distributions for reduction in canopy cover between three TEU classes, estimated in Digital Mylar.

Spatial Wavelet Analysis

Comparing SWA Settings

My selection of threshold and initial wavelet size settings for the SWA algorithm was the result of an extended trial period in which I sought to understand the performance of SWA on

this imagery. The table below (Table 4) summarizes some of the results of a comparison of a variety of threshold and wavelet size settings on one image tile. I selected this tile for analysis due to its range of canopy-cover, slope, and contrast between crowns and background. The values for number of crowns identified, mean crown diameter and canopy-cover were taken directly (or calculated from these values) from each SWA run's attribute table. I calculated the estimates of commission and omission error from ten 20 m-radius circular plots. The grey lines indicate the final settings used in this study.

Table 4. A comparison of different threshold and wavelet size settings over one image tile. The values for the number of crowns identified, commission error, and omission error were the same for each wavelet seize within a threshold setting.

Threshold & SWA Size	Total Crowns Identified	Commission Error	Omission Error	Mean Crown Diameter (m)	Canopy Cover
0 & 2 m	35566	14%	24%	0.80	3.52%
0 & 6 m				2.71	18.69%
0 & 12 m				3.36	26.83%
30 & 2 m	31956	6%	24%	0.83	3.14%
30 & 6 m				2.80	17.46%
30 & 12 m				3.45	25.34%
70 & 2 m	29364	0%	29%	0.82	2.67%
70 & 6 m				2.85	16.42%
70 & 12 m				3.49	23.51%
100 & 2 m	19986	0%	48%	0.84	1.57%
100 & 6 m				3.01	12.15%
100 & 12 m				3.75	18.20%

.

There are several aspects of SWA performance illustrated by the results of this comparison. Regarding the selection of threshold and wavelet size settings, the table indicates the following:

1. The number of crowns identified is dependent on threshold settings and not on wavelet size settings.
2. The mean crown diameters identified change with the wavelet size, but not because a different cohort of trees is identified – the same trees are identified regardless of the wavelet size setting. Changes in this setting only produce different diameter estimates.
3. At low wavelet size settings – 2 m in this comparison – the SWA algorithm attributes the majority of crowns with a diameter of 0 m.

The results of this comparison indicate that my selection of settings comprised a balance of omission error and commission error, and wavelet size. For these data, a threshold value under

30 would have increased commission error without a decrease of omission error, while a threshold value over 70 would have increased omission error without decreasing commission error. Given the omnipresence of omission error in the table above, I considered a higher omission error worth the slight reduction in commission error. SWA settings that missed crowns at a certain rate but did not invent them would be more useful for estimation of canopy-cover and legacy and non-legacy density mapping that would settings which had had moderately high levels of both error types. Similarly, changing initial wavelet size would have shifted the mean value of crown diameters accordingly without improving the ability to locate crowns. My comparison of SWA-derived and GIS-measured crown diameters below addresses the performance SWA in estimating crown diameter.

Comparison of Canopy-Cover Estimates

SWA estimates of canopy-cover proved fairly efficient (EF from 0.158 to 0.501 overall depending on SWA run and year), but systematically underestimated canopy-cover, especially as cover increased (Figure 6). Separating low canopy-cover polygons, I found that SWA-derived cover estimates fairly match Digital Mylar estimates and show low bias up to 15% canopy-cover (Table 5).

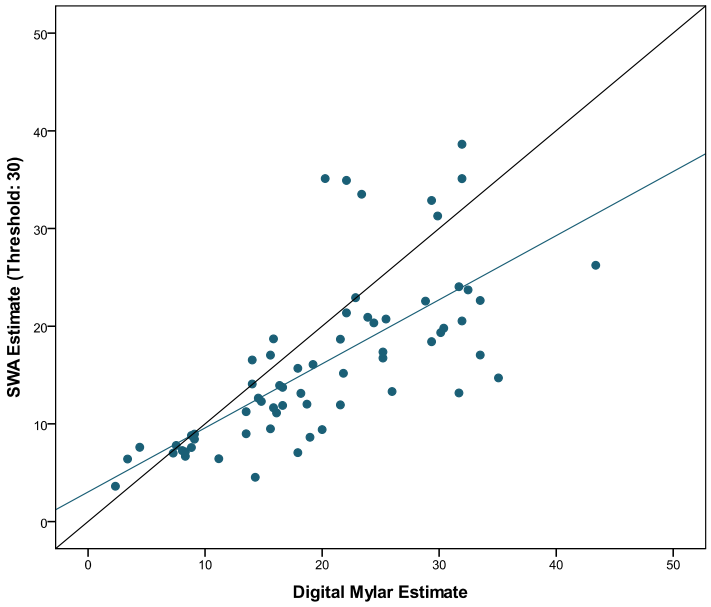

Figure 6. Comparison of canopy-cover estimates from (n = 64) TEU polygons using the 2000 30-threshold SWA run and Digital Mylar. The black line indicates a one-to-one relationship, the blue line indicates best data fit.

Table 5. Mean absolute error, mean bias error, and model efficiency statistics for all SWA canopy-cover estimates, and for SWA estimates on polygons below 15% canopy-cover.

All Polygons					
Year & Threshold	**MAE**	**MBE**	**EF**	**Pearson's r**	**Sig.**
2000 & 30	0.056	0.036	0.311	0.722	$p < 0.0001$
2008 & 30	0.050	0.029	0.501	0.782	$p < 0.0001$
2000 & 70	0.062	0.046	0.158	0.699	$p < 0.0001$
2008 & 70	0.056	0.044	0.368	0.779	$p < 0.0001$
Polygons Below 15% Canopy Cover					
2000 & 30	0.022	0.009	0.326	0.665	$p = 0.001$
2008 & 30	0.023	-0.002	0.511	0.689	$p = 0.001$
2000 & 70	0.018	0.017	0.470	0.827	$p < 0.0001$
2008 & 70	0.029	0.013	0.587	0.814	$p < 0.0001$

Comparing estimates of change between the two methods showed even greater variability, as the errors from both years confounded accurate estimation. Though the trend is discernible, many paired SWA and Digital Mylar estimates diverge greatly, and there are numerous outliers (Figure 7).

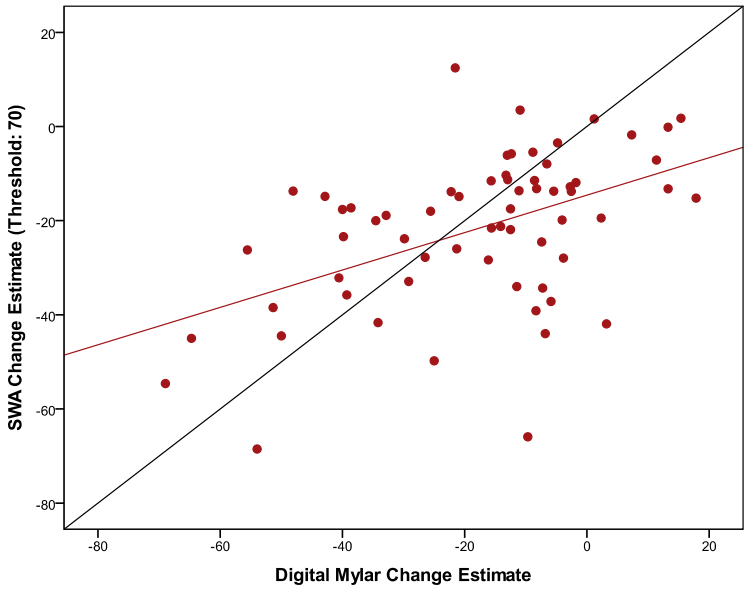

Figure 7. Comparison of canopy-cover change estimates from (n = 64) TEU polygons using both techniques. Note bias in estimates leading to overestimation of highly negative change and underestimation of moderately negative to positive change.

Comparing treatment means showed greater agreement between the two estimation types than is indicated in the above figure. Though change estimates on individual polygons often differ, there was considerable agreement in change means in burn and thin-and-burn treatments (Table 5 and Figure 8). Indeed, there is not statistical difference between these treatment means, the highest significance level suggesting a difference ($p = 0.219$) is far above my statistical cut-off of significance ($p = 0.05$). To a greater extent than with Digital Mylar canopy-cover estimates in untreated polygons, SWA estimates varied widely, from -25% to no change with a threshold of 70 and -32% to +14% with a threshold of 30. SWA untreated change estimates are statistically different from the (statistically non-significant) Digital Mylar estimate, though the amount of change is on the same order of magnitude.

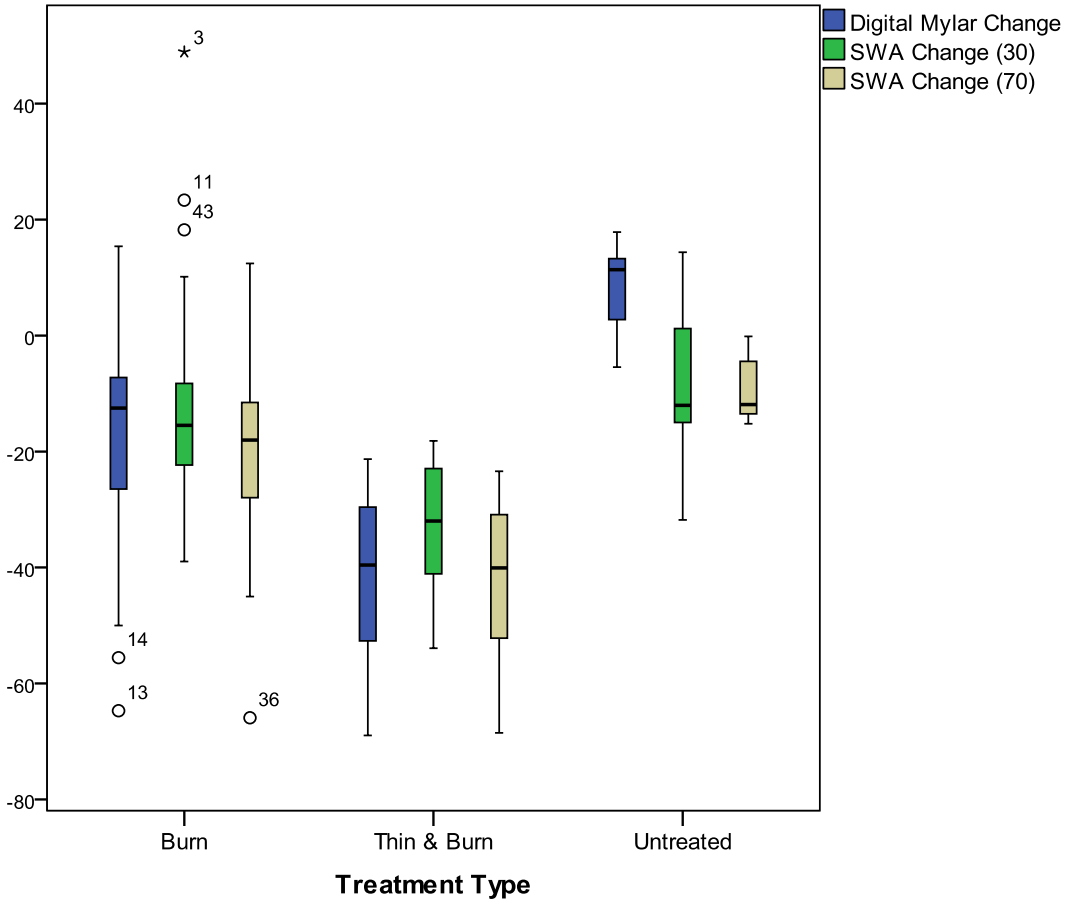

Figure 8. Means and data distributions of treatment means from Digital Mylar and SWA runs.

Crown Diameter

I measured the accuracy of SWA crown diameter estimates using 146 points identified as trees by the wavelet algorithm. As described above, estimation of tree location, diameter, and canopy-cover is most accurate in open areas, and degrades in accuracy as canopy-cover increases. Plotting these estimates together (Figure 9) shows the same heterogeneity of variance evident in the canopy-cover estimates above (Figure 6). The ability of SWA to estimate crown diameters with less overall error (compared to GIS-measured crown diameters) was higher in the open cover class (MAE = 0.963, MBE = 0.732, EF = 0.558) than in the other classes (Table 6 and Figures 9 and 10).

This point-to-point analysis also produced an estimate of commission error – that is, those points that do not overlay tree crowns, but instead some other dark (or even faintly darker) object. Commission error was highest in the open cover class (three false positives, or a seven percent commission error rate), compared to the mixed class (one false positive, two percent commission error rate) and closed cover class (two false positives, four percent commission error rate). Total commission error was four percent.

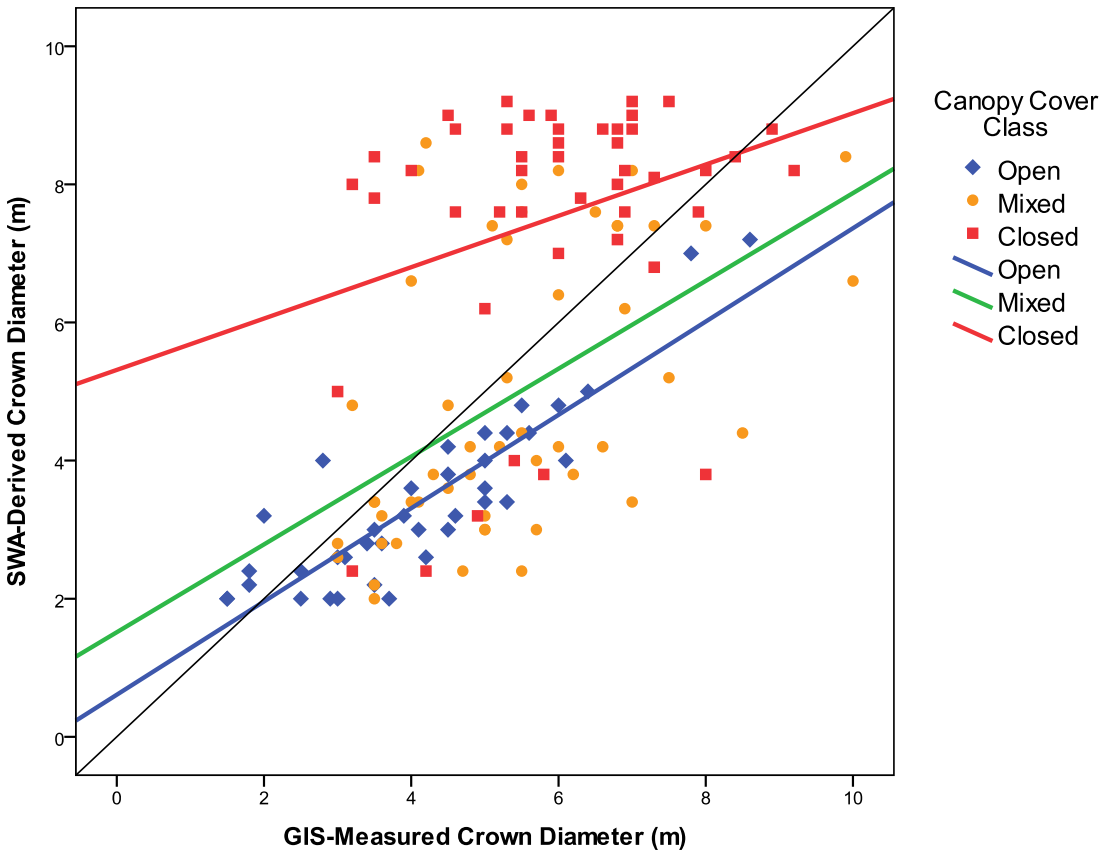

Figure 9. SWA-derived crown diameter estimates vs. GIS-measured crowns, for all cover classes. The black line represents a one-to-one line.

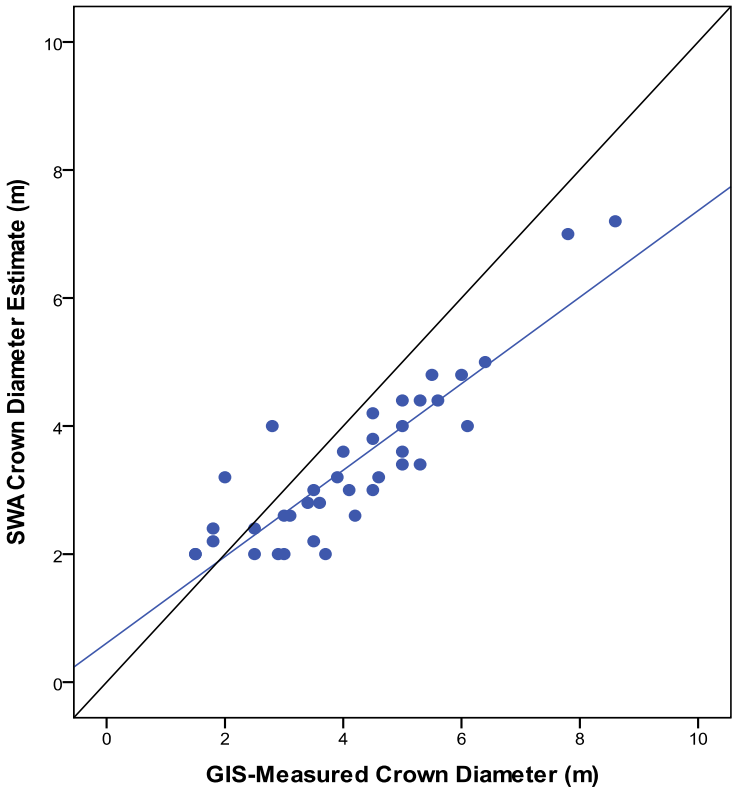

Figure 10. SWA-derived crown diameter estimates vs. GIS-measured crowns in the open cover class. Black line indicates one-to-one relationship

Table 6. Sample sizes, mean absolute and bias errors, model efficiency, and correlation statistics with significance levels for SWA crown diameter estimation in each cover class.

Cover Class	n	MAE	MBE	EF	Pearson's r	Sig.
Open	38	0.963	0.732	0.558	0.880	$p < 0.0001$
Mixed	51	1.543	0.445	-0.377	0.507	$p < 0.0001$
Closed	46	2.163	-1.563	-0.100	0.304	$p = 0.04$

To determine the rate of omission error in the SWA algorithm's identification of tree crowns, I randomly placed ten 20m-radius plots on 2000 and 2008 SWA runs for both thresholds (for a total of forty circular plots).

Omission error rates were high in both thresholds (Table 7), but were lower in open cover class than overall. I did not observe any commission errors on these forty plots. Only on a few portions of the analysis area did I observe commission error, but these areas proved sufficiently small for inclusion in my samples. Commission errors were detected in the sample of 140 SWA-identified crowns and the comparison of wavelet settings, both described above. Commission

error occurrence was highly variable, but based on the estimates above seems to be between four and six percent.

Table 7. Omission errors overall and in the open cover class for SWA tree identification in both threshold settings

SWA Threshold	Overall Omission Error	Open Cover Class Omission Error
30	62%	32%
70	70%	40%

Crown Diameter Distribution

I used the virtual census produced by SWA and a sample of GIS-measured crown diameters to examine crown diameter frequencies across the landscape and assess the ability of SWA to estimate this basic forest characteristic on a landscape scale. Using the forty 20 m-radius plots described above, I created histograms of GIS-measured crown diameters for both years (Figures 11a and b).

These histograms appear roughly symmetrical, with means of 2.96 m $\pm$ 0.09 m and 3.19 m $\pm$ 0.08 m crown diameter. The tailing off of frequency at the larger tree diameters may indicate multiple crowns forming a continuous, seemingly singular crown.

I randomly sampled 146 identified points from the 70-threshold 2000 and 2008 SWA runs to produce histograms of their crown diameter estimates. The results show a marked difference from the histograms above (Figures 11c and d). Both years display bimodal distributions with means between the two peaks in the distribution (5.9 m $\pm$ 0.20 m and 5.57 m $\pm$ 0.21 m respectively).

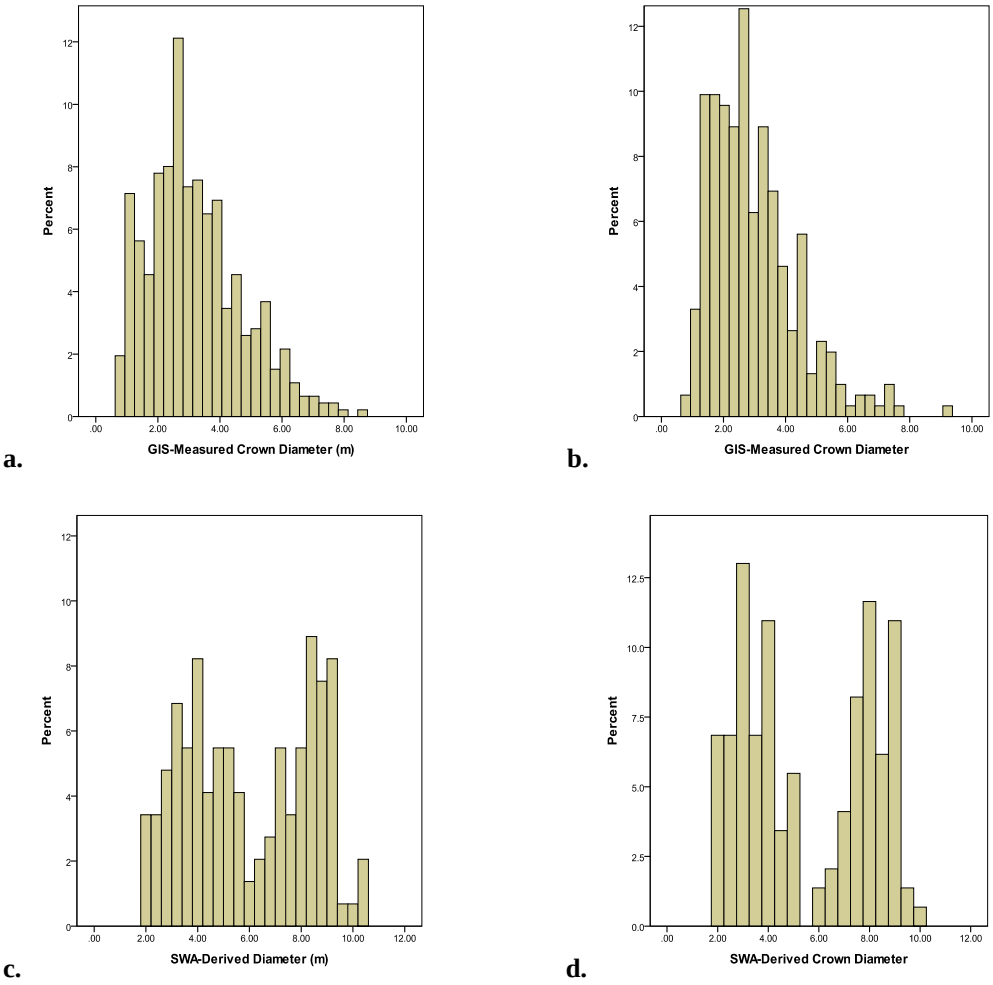

Figures 11a through d. Histograms of GIS-measured crown diameters in from 2000 imagery (a) and 2008 (b). Figures 11c and d depict SWA crown diameters in 2000 and 2008. Note normal distribution of GIS-measured diameters and bimodal distribution of SWA diameters.

Legacy and Expansion Trees

Finally, I strove to investigate the locations and concentrations of "legacy trees" – those old growth trees which would characterize the historical forest condition prior to Euro-American settlement and official government land management practices. I defined a legacy tree in the context of SWA results as those crowns with diameters from 6 meters to 10 meters, as they represented the right tail of the distribution of GIS-measured crown diameters (Figures 11a and b). This necessarily differs from Clifton's definition of a legacy tree (Diameter at root collar > 24 cm) as crown diameter is the only metric available from aerial imagery. I sampled legacy trees in both the 30- and 70-threshold SWA runs. I first randomly selected 50 crowns in the open from each of four diameter classes – 6 to 6.8 m, 7 to 7.8 m, 8 to 8.8 m, and 9 to 10 m – to determine if

different classes of legacy trees were more likely to have been correctly identified as legacy trees. I expected a steady improvement in SWA's ability to correctly identify crowns in the legacy category as diameter increased (an incorrect identification in this case includes both identifying a tree that is not present, or identifying a tree whose canopy is under 6m in diameter a legacy tree). Instead, in the 70-threshold run, all classes correctly identified legacy trees at similarly high rates: 74 $\pm$ 6.3% of the time for the 8 to 8.8m class, and 80 $\pm$ 5.7% of the time for the other classes. Ignoring size classes, accuracy of all 70-threshold run legacy tree estimates was 79 $\pm$ 2.9%.

The second sample I took to determine the viability of a legacy tree map was on 100 randomly selected open-grown crowns in from the entire range of legacy tree diameters (6 to 10m) from the 30-threshold SWA run. As expected, the ability to correctly identify trees was diminished in this less discriminating run, but the accuracy for the group was 68 $\pm$ 4.7%.

Though the 70-threshold SWA run had a higher accuracy rate (79% vs. 68%) than the 30-threshold run, I used the latter for legacy tree mapping. The higher omission error associated with the higher threshold resulted in small areas of the image where trees were not identified, and therefore erroneous values in the density maps. Omission rates for these two thresholds estimated on plots above were 40% in open areas for 70-threshold runs and 32% in open areas for 30-threshold runs. Figures 12 and 13 display legacy tree crowns identified by the 2000 SWA 30-threshold run.

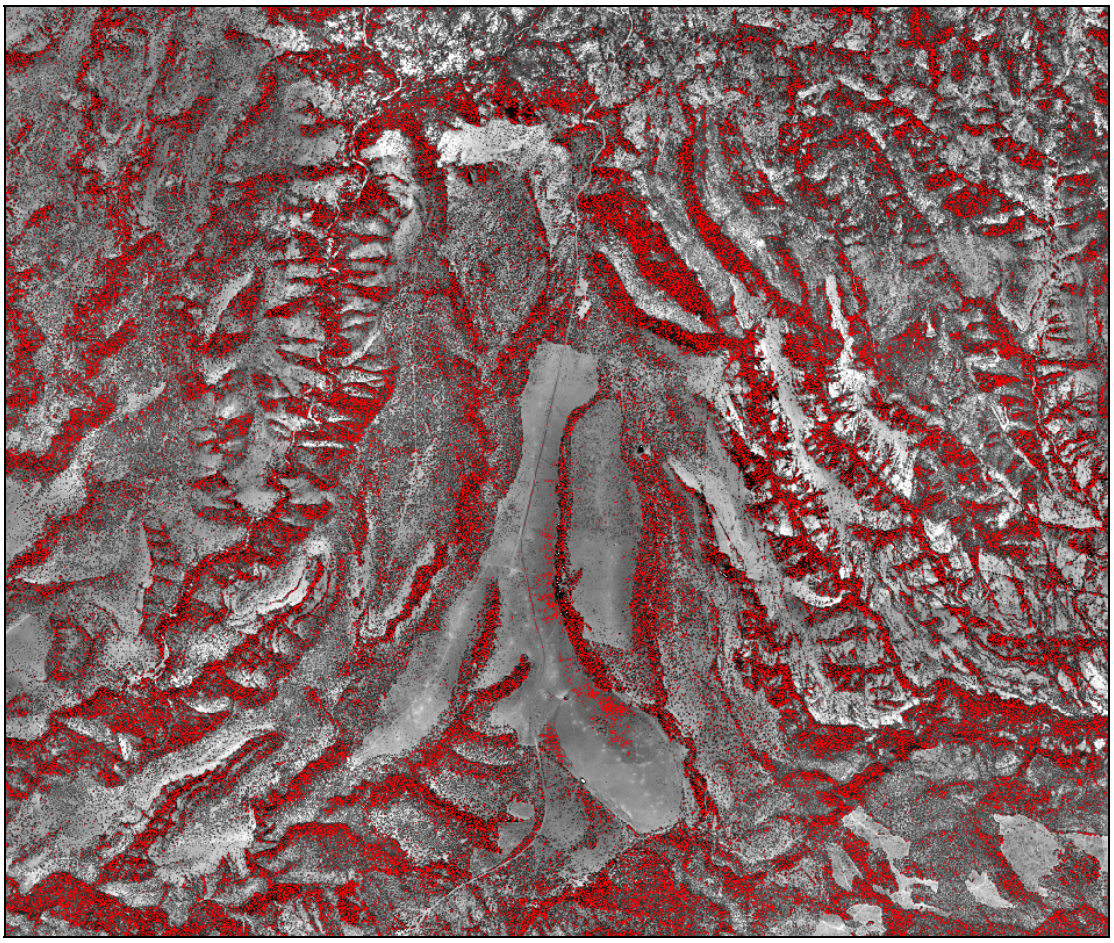

Figure 12. SWA-defined legacy trees overlaying 2000 aerial imagery of Mesa project area.

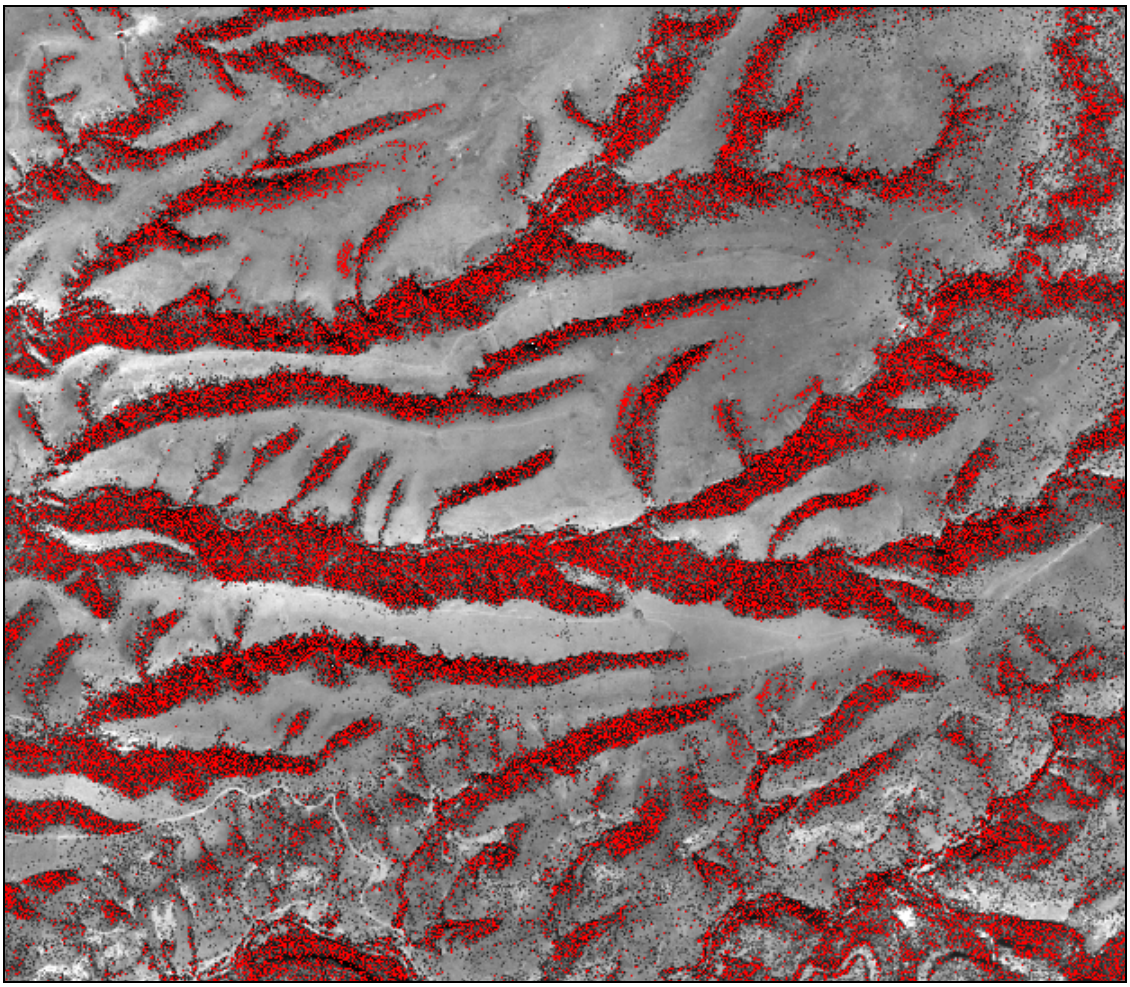

Figure 13. SWA-defined legacy trees overlaying 2000 aerial imagery of the western portion of the NO Bar project area.

Using legacy trees and non-legacy trees separately, I used the Spatial Analyst® extension to ArcGIS® to create raster images representing densities of legacy trees and non-legacy trees. I used a kernel of 50m in radius to produce pixel values. This mismatched kernel area and output pixel size creates a smoothed image of trends in center point densities. Such a smoothed image displays a generalized picture of relative tree densities without attempting to show exact locations of every tree.

On the following pages are density images of juniper expansion patterns (Figures 14, 16 and 17) and a set of figures showing the similarity between aerial photography and SWA wavelet results (Figures 15a through d).

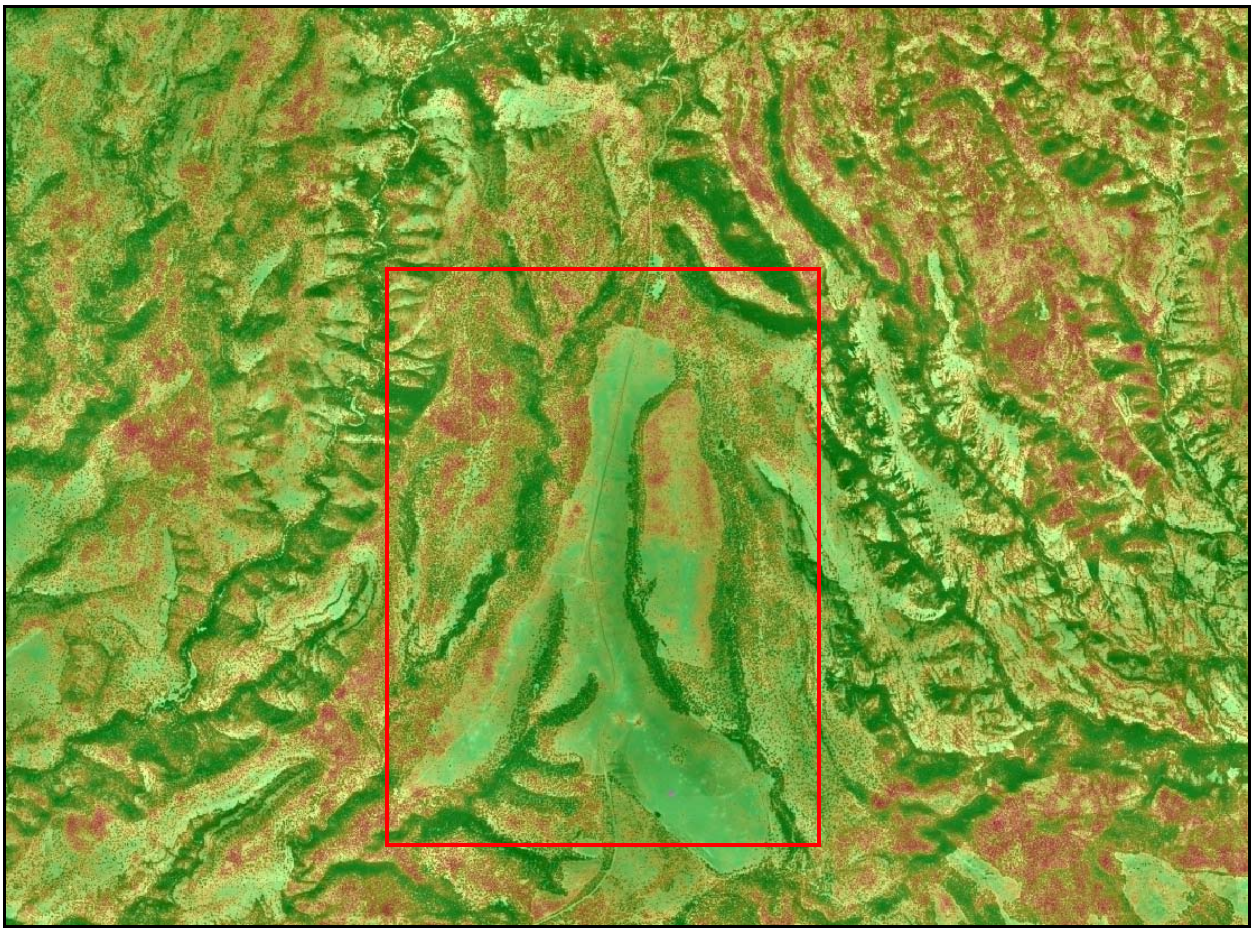

Figure 14. A 50m pixel density image representing non-legacy tree, “juniper invasion” tree concentrations on a portion of the Mesa area in 2000. Values range from zero tree centers per ha (green areas) to 6100 tree centers per ha (red areas).

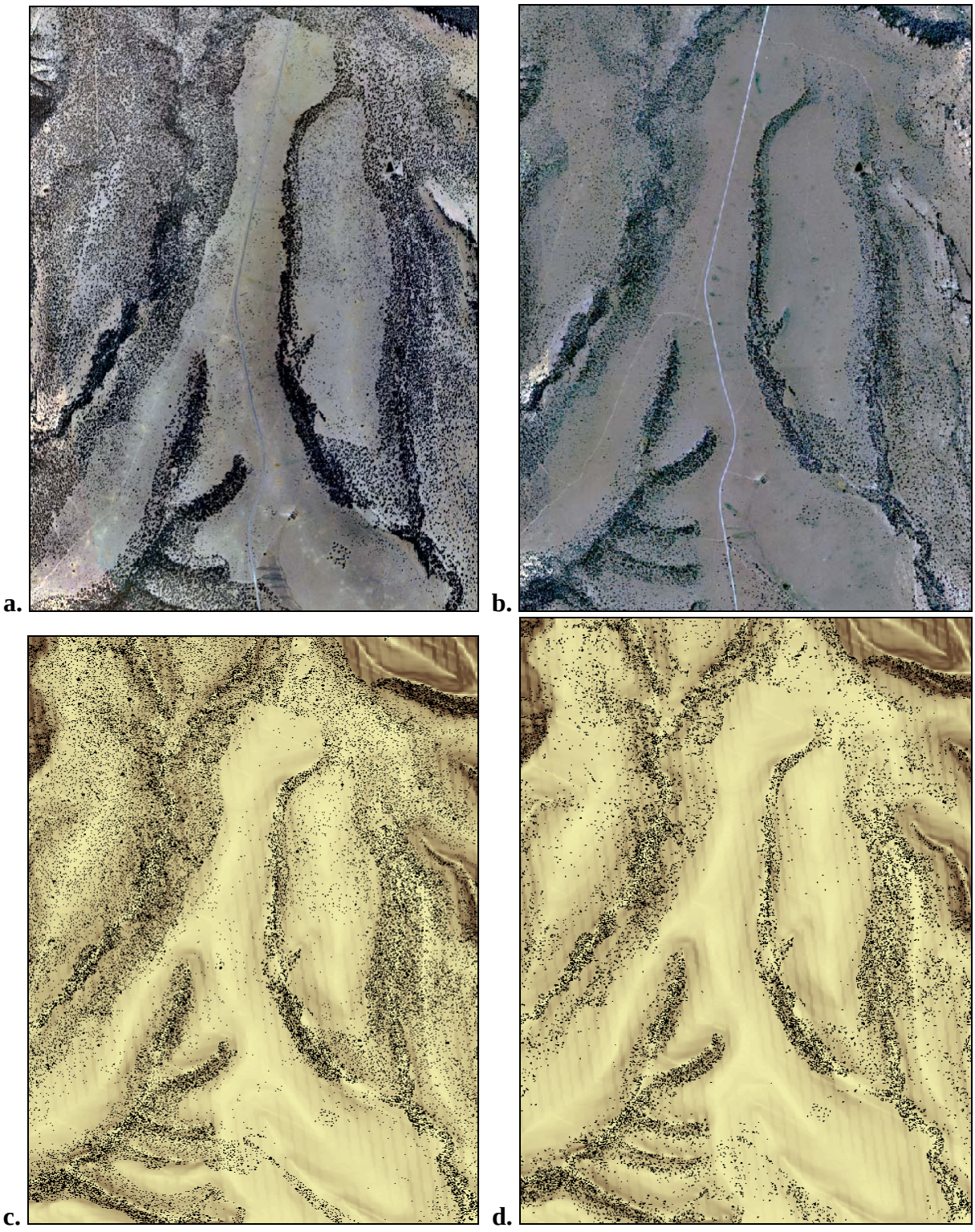

Figures 15a through d. Figures 15a and b (aerial images from 2000 and 2008) depict the red-boxed area in Figure 14 above pre- and post-treatment. Note the change in tree density on mesa tops following treatment.
Figures 15c and d depict the above area with all 2000 SWA trees (c) and only SWA legacy trees (d) The SWA trees overlay a slope image derived from a DEM. Note the similarities between in tree densities, and the similarity between the legacy tree image and the 2008 post-treatment image (b).

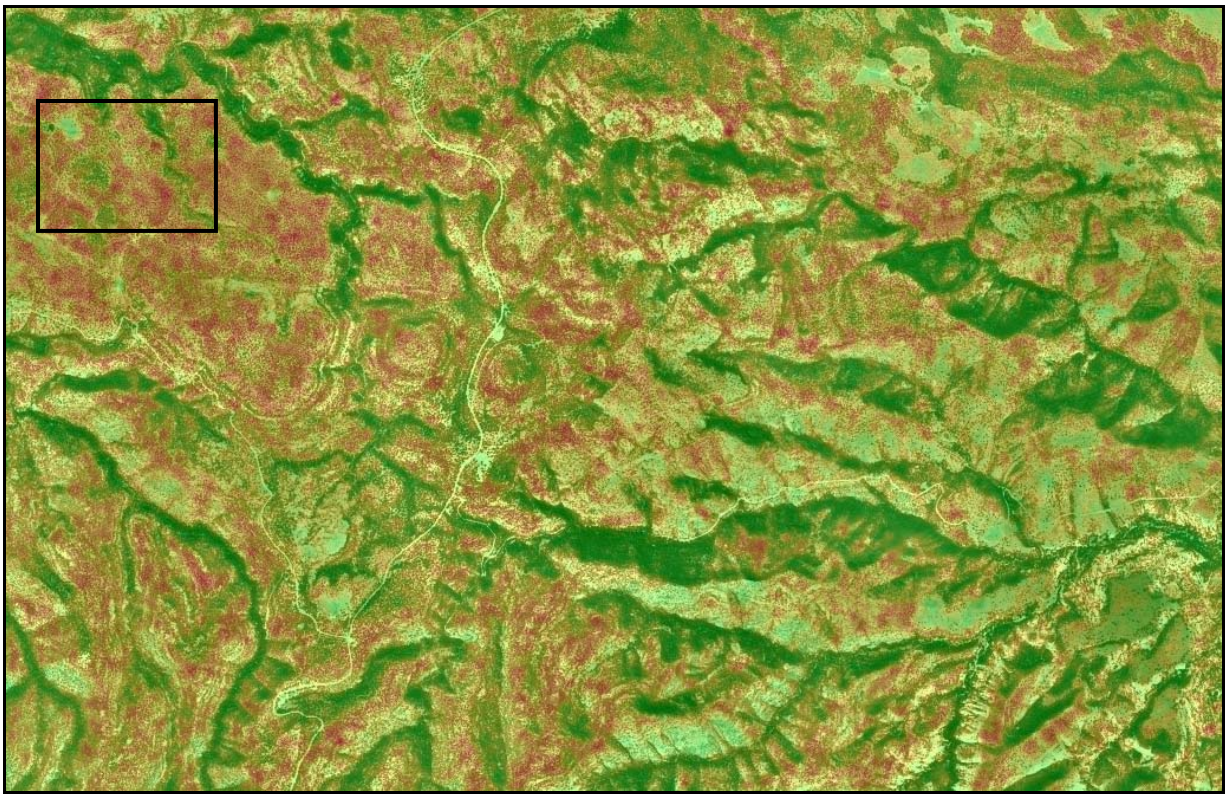

Figure 16. A 50 m density image representing non-legacy tree concentration on a portion if the NO Bar area in 2000. Higher densities (in orange and red) reach a maximum of 6100 tree centers per ha. The black-boxed area in the upper left is shown in Figure 17 below.

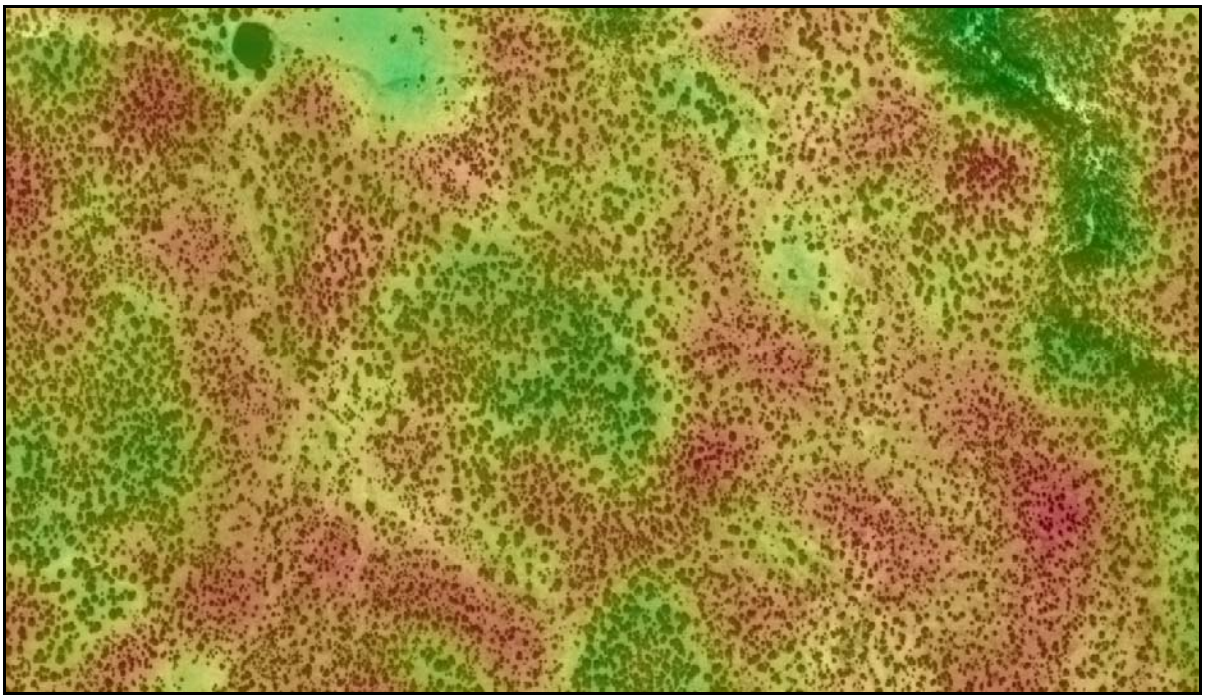

Figure 17. A zoomed-in view of the black-boxed area in Figure 16, allows the viewer to compare areas of rampant juniper invasion (in orange and red) to areas of low invasion (in green). Note that the low invasion areas either show very few tree crowns, or may have a higher density of legacy tree crowns.

Discussion

Restoration Treatments

Both burn and thin-and-burn treatments were shown to produce statistically significant reductions in canopy-cover. A separation of polygons by the general topographic type they overlay (mesa top, draw, and mixed) allowed for a comparison of topographically similar polygons, and to quantify the effect of topography on canopy-cover reduction. This categorization showed that no thin-and-burn treatments were carried out in draws, which is logical considering the vegetation density and steep terrain of draws in this landscape. Comparing mesa top and mixed burn treatments with mesa top and mixed thin-and-burn treatments showed non-significantly higher canopy-cover reduction in thin-and-burn polygons in both topographic types. Given the small sample sizes for thin-and-burn statistics when broken up into topographic types ($n = 4$ for each type), and the relatively low p-values ($p = 0.07$ and 0.06 for mesa top and mixed, respectively), it is possibly reasonable to assume thin-and-burn canopy-cover reduction is greater even when categorized by topographic type. This analysis shows, however, that topography is an important factor in affecting canopy-cover reduction from prescribed burning.

Comparing post-treatment canopy-cover estimates with a target canopy-cover value of under 15%, we find again that thin-and-burn treatments reduce canopy cover to target levels more often than burn treatments, even though the starting average canopy-cover for thin-and-burn polygons was greater. This treatment, which provides added fuel for higher-intensity fire and reduction of canopy-cover from stem removal, proves a highly effective way to reduce canopy-cover to target levels. The increased cost of such treatments – almost ten times more expensive per hectare – calls for thoughtful, limited implementation given budget constraints.

TEU Type and Fire Effects

This study found no evidence to support the assertion that fire effects in indicated TEU type 632 (Lithic Argiustolls on generally steeper slopes), are substantially greater than those in types 589 and 630 (Vertic and Lithic Argiustolls on generally gentler slopes). Without a very large sample size, in-depth knowledge of fire effects observed, prescribed fire lighting patterns, and other factors affecting burn intensity and severity, I do not report this disagreement between

data and expert opinion as conclusive. My analysis indicates that any perceived differences in fire effects may be illusive, or not universal for all TEU types indicated across the landscape. Based on this study, guiding treatments based on TEU type seems suspect without further data indicating the proposed relationship exists.

Digital Mylar Effectiveness and Results

The initial favorable expectations of the viability of Digital Mylar as a means of measuring forest change proved well-founded. I found that with a brief introduction and training period, and with consistent rules in determining crown "hits" and "misses," analysis of numerous discrete areas proved both easy and efficient. It is important that the areas being measured are relatively uniform in canopy-cover, and do not contain great variability within each discrete unit. Clumps of canopies distributed throughout the analysis unit would require the use of a systematic grid instead of the randomly placed sample points used in this study. Digital Mylar's user-friendly interface allows for either of these sampling schemes.

After I tallied preliminary results for each project area using Digital Mylar, I assisted Clifton Ranger District personnel in adopting the process for future technical reports and management planning. The quick adoption of the method speaks to its utility as a monitoring and planning tool.

Digital Mylar-produced change estimates for both burn and thin-and-burn units were not surprising given the nature and intent of the treatments. Upon reflection, the non-significant finding of change in untreated polygons is likewise not surprising. In an arid, minimally productive environment, an eight year interval between estimates proved insufficient to measure change on the landscape through the growth of new stems. In extrapolating change data from other studies in arid or semi-arid juniper environments, an annual expansion/infill addition to canopy-cover of around 1% (e.g. 10% to 11% canopy-cover would be an addition of 1%) appears plausible (Goslee et al. 2003, Sankey et al. 2008). Goslee et al. (2003) also reveals, however, a non-linear increase in shrub canopy-cover in New Mexico over 60 years. Per annum canopy-cover additions ranged from 0.7% to 5.2%, and decreases in cover were also observed. Without more definite findings in this study, however, I am wary of drawing many inferences from these data.

Spatial Wavelet Analysis Effectiveness and Results

SWA as an Analysis Tool

The data preparation requirements, analysis process, and results of SWA all differ greatly from those of Digital Mylar analysis. Without a user-friendly interface of any kind, the algorithm used in this study would prove very difficult to learn in a reasonably short amount of time. Altering the algorithm to produce output files of a different type suitable for a user's purposes would require a considerable devotion of time and energy to learn the basics of the MATLAB programming language and the specific functions of individual parts of the SWA algorithm. In my case, the process of understanding the language and this algorithm included one-on-one mentoring with experienced programmers, extensive reading, and most importantly, an extended period of trial-and-error occasioned by considerable frustration and infrequent, minor breakthroughs.

Beyond the initial extended training process, SWA presents several unique challenges to the user. First, although SWA provides the ability to process imagery depicting a potentially limitless geographic area, the process is not scalable in the same way as Digital Mylar. Given a level of uniformity of the analysis features on the landscape, estimation with Digital Mylar is possible for vast areas. Analysis with SWA requires breaking imagery into relatively small pieces and processing them sequentially, adding a significant step in image pre-processing.

Second, the SWA algorithm in its current form does not calculate canopy-cover. The list of features with their associated locations and radii initially seems to allow a simple mathematical calculation of total feature area, but is confounded by the tendency of the algorithm to define overlapping canopies, especially (but not only) where canopy-cover increases. The user must therefore further manipulate the data to produce estimates of canopy-cover (as I did in dissolving canopies together and calculating the resulting area in ArcGIS).

Third, the quantity of data provided by SWA can prove overwhelming. Even given the high omission rates over much of the analysis area, each SWA run over the entire series of image tiles produced a total of 700,000 to 1 million records. Though this data represents a virtual census (bearing in mind considerable omission and commission errors) of all tree crowns in the analysis area, the accuracy of this census requires further sampling of the data. Indeed, I found it necessary to sample SWA data even in producing a histogram of SWA-derived crown diameters, as processing demands for such quantities of data proved unwieldy or impossible.

SWA Estimates

The documented inability of the SWA algorithm to reliably locate and properly attribute tree crowns at canopy-cover rates approaching 25% (Strand et al. 2006) proved a major factor in the analysis of my study area. I found that with my imagery and manipulation of the SWA algorithm, about 15% proved to be the cutoff for particularly accurate estimates of crown size.

In partially closed and closed canopy areas, the tendency was for the SWA to define large areas, particularly shadows, as tree crowns. The SWA algorithms acts consistently enough, however, that in closed canopy environments change estimates were consistent with Digital Mylar estimates either in their actual value, or at least the magnitude and direction of change. Consequently, despite high omission error and a general breakdown in closed canopy areas, treatment means for burn and thin-and-burn polygons proved statistically equivalent.

To a greater extent than discussed by Strand (2007) and Strand, et al. (2006 and 2008), I found that shadows from even open-grown, well-defined juniper crowns were problematic for SWA in determining crown diameter. In many cases, the SWA identified the shadow, and the quality of its estimate of crown diameter was hostage to the correlation of each individual crown's shadow size to its diameter. This tendency explains the underestimation of both crown diameter and canopy-cover. Only in cases where illumination and slope factors caused the shadow to fall directly under the tree did SWA precisely delineated the center point and spatial extent of the tree crown.

Strand (2007) describes the inability of SWA to identify crowns with diameters smaller than 2 m to 3 m. This study found that SWA does tend to underestimate the prevalence of trees in this size class (compare crown diameter histograms from SWA in Figures 14 and 15 with GIS-measured diameters in Figures 12 and 13), but did indeed identify thousands of them on the landscape. Examining these histograms, one should note the presence of two other phenomena. First is the bell-shaped, relatively symmetrical distribution of the GIS-measured crown diameters. Baker (2009) explains that, "[pinon-juniper woodlands] 100-200 years old often have a bell-shaped age structure, as a cohort of trees recovered after disturbance…" It may therefore be reasonable to conclude that some substantial subset of the study area falls into this age range, assuming a correlation between crown diameter and tree age.

The second phenomenon is the bimodal distribution of both SWA histograms of crown diameter. Not only does this distribution have the effect of shifting the mean significantly higher

than the GIS-measured mean, but it again reveals the effect of SWA's unreliability to estimate crown diameter in closed-canopy areas. This peak of large diameter crowns centered around 8m overwhelmingly represents draws and other closed-canopy areas, where SWA identified large areas of shade as enormous tree crowns.

Legacy and Expansion Tree Locations and Densities

Bearing in mind the accuracy rates of open-grown legacy tree identification (68% for 30-threshold and 79% for 70-threshold SWA runs), images produced as generalized analogs for historic condition (Figures 11 and 12) and juniper expansion (Figures13 and 15) indicate some ecological characteristics of particular interest to managers pursuing landscape restoration goals. As one might expect, draws and canyons contain the preponderance of legacy trees. In previous centuries, it appears few trees occupied the mesa tops, and these areas maintained a very open condition.

These images also indicate that in areas of extensive shading and continuous crown cover legacy tree identification is unrealistically high. Because SWA is so unreliable in such conditions, and crown diameter measurement is difficult even with the naked eye, I did not measure the accuracy of legacy tree identification in closed canopy or highly-shaded areas. Use of the density images above, therefore, should be thoughtfully undertaken, and include accuracy assessment for particular areas of interest to users.

Conclusions and Management Implications

In this study, I intended to both provide estimates of restoration treatment efficacy, and evaluate the utility of two estimation methods. I examined canopy-cover pre- and post-treatment and compared these results with adjacent untreated areas. I compared Digital Mylar and SWA estimation methods, and explored further analysis using SWA data, including a characterization of vegetation structure, and imagery illustrating legacy and non-legacy tree locations and densities.

Restoration treatments implemented by Clifton Ranger District fire personnel significantly reduced canopy-cover, but efficacy is somewhat dependent on the topography of the burned area and the cost of treatment. The significant reduction in canopy-cover from

burning alone is promising given its low per-ha cost, but its ability to reduce canopy-cover to target levels is limited. Repeated prescribed burning treatments with similar effects, however, would reach targets over time at a fraction of the cost of a single thinning-and-burning treatment. Thinning juniper stems and burning the residue in addition to natural fuels produces great reduction in canopy-cover and appears more likely to reduce cover to target levels – but at a cost that is ten times that, per ha, of burning alone.

Given the tendency of alligator juniper to re-sprout after disturbance, repeated treatment will likely be necessary. If understory vegetation productivity increases as a result of burning alone, repeated prescribed burns may produce greater reductions in canopy-cover in the succeeding years. Estimation of understory production is beyond the scope of this study, and likely would require field sampling or multi-spectral image analysis (or both). In the long run, a scientifically-based treatment prioritization system (possibly a variant of the current TEU type system) could direct costly thin-and-burn treatments where they are most needed and will prove most cost-effective.

It is hard to impeach the quick, reliable, statistically sound estimation technique Digital Mylar represents. The process is easy to teach, is fundamentally easy to understand and does not rely on higher mathematics. Once trained, any technician can produce accurate, usable estimates of canopy-cover and change in cover. Further, it is not nearly as dependent on image quality as an image analysis algorithm, so imagery in any spatial resolution fine enough to allow discernment of individual crowns can be quickly utilized without a need for image resampling. In this manner historic images of any time period can be used as a basis for estimating cover change over long time periods. The method's one substantial downside is the time requirement involved in producing estimates in numerous areas. For the canopy-cover estimates used in this study, I looked at about 25,000 individual points. This process took about 50 total hours, spread out over two weeks.

Spatial Wavelet Analysis, on the other hand, presents unique challenges (described in the Discussion section above) to widespread implementation in a non-academic setting. Complex mathematics do not necessarily need to limit the use of SWA, as many functions in common image processing and GIS software are performed daily by users without technical understanding of their operation, or underlying theory. An interface which allows users to upload images, set thresholds and parameters and produce useful output in a user-friendly graphical environment

would drastically increase the utility of this tool among academics, researchers, and managers alike. With constraints in budget, equipment, and personnel, the time commitment and technical ability required to effectively use SWA is, at the present time, unrealistic for use in monitoring activities for land managers in most situations.

Despite these challenges and with accuracy caveats in mind, SWA provided a vast quantity of high quality data. Under certain conditions of open forest cover and quality imagery, SWA presents the opportunity of obtaining a virtual census of tree (or shrub) locations and crown diameters over a potentially vast landscape. The legacy tree and non-legacy tree images (Figures 11 through 16) are one example of a possible utility for such data. Though not a true census of juniper expansion or of legacy tree locations on the landscape, the images provide a potential guide to managers seeking an analog of historic conditions. Managers interesting in landscape restoration could use such images (with further sampling or ground-truthing for accuracy assessment of particular areas) to determine which areas appear the most departed from historic conditions and conduct treatments accordingly.

Investigation into the use of SWA data in questions of ecology, wildlife habitat potential, monitoring of management actions, and a wide variety other fields is at its beginning. The potential for performing analysis on an analog of reality, rather than a subset selected in sampling, is an exciting prospect. I expect that with further research, and the incorporation of this technique into standard image processing and/or GIS software packages, the utility of SWA will become further realized and streamlined.

Appendices

Appendix A. Polygon ID, TEU type, treatment type, Digital Mylar canopy hits, canopy-cover, and canopy-cover change estimates categorized by treatment and TEU type in the Mesa project area.

Mesa Unit

Polygon	TEU type	Treatment	2000 canopy hits	2000 CC	2008 canopy hits	2008 CC	CHANGE
18262	630	Burn	64	16.62	56	14.55	-12.50
13433	514	Burn	85	22.08	73	18.96	-14.12
16235	632	Burn	69	17.92	41	10.65	-40.58
13705	630	Burn	55	14.29	36	9.35	-34.55
13208	630	Burn	77	20.00	54	14.03	-29.87
12828	630	Burn	100	25.97	50	12.99	-50.00
13424	514	Burn	129	33.51	102	26.49	-20.93
16029	589	Burn	69	17.92	64	16.62	-7.25
16100	582	Burn	73	18.96	71	18.44	-2.74
16250	632	Burn	122	31.69	107	27.79	-12.30
18263	573	Burn	43	11.17	44	11.43	2.33
18278	582	Burn	52	13.51	50	12.99	-3.85
18274	575	Burn	122	31.69	114	29.61	-6.56
18275	514	Untreated	98	25.45	111	28.83	13.27
16244	630	Untreated	113	29.35	128	33.25	13.27
17842	130	Untreated	111	28.83	109	28.31	-1.80
14849	60	Untreated	167	43.38	186	48.31	11.38
16079	514	Untreated	92	23.90	87	22.60	-5.43
13342	512	Untreated	56	14.55	66	17.14	17.86
18267	573	Burn/Thin	29	7.53	9	2.34	-68.97
13703	630	Burn/Thin	117	30.39	77	20.00	-34.19
15350	575	Burn/Thin	123	31.95	74	19.22	-39.84
15951	632	Burn/Thin	74	19.22	36	9.35	-51.35
14596	630	Burn/Thin	84	21.82	51	13.25	-39.29
13340	630	Burn/Thin	63	16.36	29	7.53	-53.97
12831	630	Burn/Thin	60	15.58	45	11.69	-25.00
14842	589	Burn/Thin	61	15.84	48	12.47	-21.31

Appendix B. Digital Mylar canopy hits, canopy-cover, and canopy-cover change estimates categorized by treatment and TEU type in the NO Bar project area.

NO Bar Unit

Polygon	TEU	Treatment	2000 canopy hits	2000 CC	2008 canopy hits	2008 CC	CHANGE
12708	630	Burn	97	25.19	89	23.12	-8.25
13209	481	Burn	13	3.38	15	3.90	15.38
13312	514	Burn	135	35.06	105	27.27	-22.22
13579	481	Burn	28	7.27	16	4.16	-42.86
13700	60	Burn	125	32.47	119	30.91	-4.80
13702	432	Burn	57	14.81	35	9.09	-38.60
13704	481	Burn	62	16.10	52	13.51	-16.13
14602	481	Burn	34	8.83	12	3.12	-64.71
14604	481	Burn	17	4.42	16	4.16	-5.88
15143	220	Burn	54	14.03	47	12.21	-12.96
15352	589	Burn	35	9.09	21	5.45	-40.00
14844	589	Burn	9	2.34	4	1.04	-55.56
14600	589	Burn	32	8.31	28	7.27	-12.50
15141	483	Burn	35	9.09	32	8.31	-8.57
14893	630	Burn	64	16.62	57	14.81	-10.94
17491	130	Burn	88	22.86	82	21.30	-6.82
14591	582	Burn	83	21.56	72	18.70	-13.25
14592	620	Burn	78	20.26	76	19.74	-2.56
14594	481	Burn	32	8.31	27	7.01	-15.63
14598	620	Burn	115	29.87	100	25.97	-13.04
15115	632	Burn	54	14.03	50	12.99	-7.41
15118	630	Burn	129	33.51	96	24.94	-25.58
15145	620	Burn	85	22.08	86	22.34	1.18
16095	632	Burn	90	23.38	80	20.78	-11.11
16098	482	Burn	31	8.05	28	7.27	-9.68
15351	130	Burn	94	24.42	97	25.19	3.19
15412	632	Burn	113	29.35	103	26.75	-8.85
16845	620	Burn	123	31.95	118	30.65	-4.07
16847	482	Burn	60	15.58	55	14.29	-8.33
16097	220	Burn	61	15.84	54	14.03	-11.48
15122	622	Burn	97	25.19	85	22.08	-12.37
15123	589	Burn	72	18.70	51	13.25	-29.17
16094	481	Burn	34	8.83	25	6.49	-26.47
13296	634	Burn	116	30.13	91	23.64	-21.55
17203	630	Burn	52	13.51	27	7.01	-48.08
17850	630	Burn	70	18.18	47	12.21	-32.86
18004	512	Burn	83	21.56	70	18.18	-15.66
14875	620	Untreated	123	31.95	132	34.29	7.32

Appendix C. 2000 and 2008 sample sizes, canopy-cover and canopy-cover change for each TEU type across both project areas.

TEU	TREATMENT	Canopy Hits 2000	n	Canopy Hits 2008	n	2000 CC	2008 CC	CHANGE
60	BURN	125	385	119	385	32.47	30.91	-4.80
130	BURN	182	770	179	770	23.64	23.25	-1.65
220	BURN	115	770	101	770	14.94	13.12	-12.17
432	BURN	57	385	35	385	14.81	9.09	-38.60
481	BURN	220	2695	163	2695	8.16	6.05	-25.91
482	BURN	91	770	83	770	11.82	10.78	-8.79
483	BURN	35	385	32	385	9.09	8.31	-8.57
512	BURN	83	385	70	385	21.56	18.18	-15.66
514	BURN	349	1155	280	1155	30.22	24.24	-19.77
573	BURN	43	385	44	385	11.17	11.43	2.33
575	BURN	122	385	114	385	31.69	29.61	-6.56
582	BURN	208	1155	193	1155	18.01	16.71	-7.21
587	BURN	41	385	22	385	10.65	5.71	-46.34
589	BURN	217	1925	168	1925	11.27	8.73	-22.58
620	BURN	401	1540	380	1540	26.04	24.68	-5.24
622	BURN	97	385	85	385	25.19	22.08	-12.37
630	BURN	708	3465	512	3465	20.43	14.78	-27.68
632	BURN	448	1925	381	1925	23.27	19.79	-14.96
634	BURN	116	385	91	385	30.13	23.64	-21.55

TEU	TREATMENT	Canopy Hits 2000	n	Canopy Hits 2008	n	2000 CC	2008 CC	CHANGE
60	UNTREATED	167	385	186	385	43.38	48.31	11.38
130	UNTREATED	111	385	109	385	28.83	28.31	-1.80
512	UNTREATED	56	385	66	385	14.55	17.14	17.86
514	UNTREATED	190	770	198	770	24.68	25.71	4.21
620	UNTREATED	123	385	132	385	31.95	34.29	7.32
630	UNTREATED	113	385	128	385	29.35	33.25	13.27

TEU	TREATMENT	Canopy Hits 2000	n	Canopy Hits 2008	n	2000 CC	2008 CC	CHANGE
573	BURN/THIN	29	385	9	385	7.53	2.34	-68.97
575	BURN/THIN	123	385	74	385	31.95	19.22	-39.84
589	BURN/THIN	61	385	48	385	15.84	12.47	-21.31
630	BURN/THIN	324	1540	202	1540	21.04	13.12	-37.65
632	BURN/THIN	74	385	36	385	19.22	9.35	-51.35

Appendix D. SWA-derived canopy-cover estimates for TEU polygons in the Mesa project area. Crown area and polygon area are both recorded in square meters.

	2000					2008					
	30threshold			70threshold		30threshold			70threshold		
Polygon ID	Crown (m2^)	Polygon Area	Cover%	Crown	Cover	Crown	Cover	Change	Crown	Cover	Change
18262	156146.09	1136215.68	13.74	149824.39	13.19	133925.52	11.79	-14.23	123617.93	10.88	-17.49
13433	165572.54	775110.53	21.36	160217.18	20.67	134909.70	17.41	-18.52	126195.51	16.28	-21.23
16235	447246.44	2851332.80	15.69	423847.15	14.86	332642.59	11.67	-25.62	287553.33	10.08	-32.16
13705	11721.03	258388.86	4.54	19779.40	7.65	17454.02	6.75	48.91	15822.33	6.12	-20.01
13208	41850.07	444562.07	9.41	47366.75	10.65	40009.94	9.00	-4.40	36071.19	8.11	-23.85
12828	49526.10	372045.01	13.31	47616.87	12.80	32852.72	8.83	-33.67	26434.35	7.11	-44.49
13424	489622.93	2163289.85	22.63	470797.55	21.76	426409.41	19.71	-12.91	400730.37	18.52	-14.88
16029	12495.59	177194.55	7.05	19061.94	10.76	13762.82	7.77	10.14	12518.04	7.06	-34.33
16100	53214.90	616436.76	8.63	69260.54	11.24	65644.80	10.65	23.36	60400.58	9.80	-12.79
16250	13381.07	101647.52	13.16	6401.45	6.30	16335.67	16.07	22.08	15015.01	14.77	134.56
18263	17544.33	272679.18	6.43	15881.74	5.82	13906.81	5.10	-20.73	12793.93	4.69	-19.44
18278	29311.19	249227.08	11.76	27704.32	11.12	19687.31	7.90	-32.83	18933.20	7.60	-31.66
18274	163555.65	680323.53	24.04	161702.86	23.77	153313.24	22.54	-6.26	148840.49	21.88	-7.95
18275	1386958.67	6691029.19	20.73	896510.54	13.40	945837.40	14.14	-31.80	895154.62	13.38	-0.15
16244	40112.15	122022.83	32.87	39990.72	32.77	35287.96	28.92	-12.03	34700.72	28.44	-13.23
17842	816171.42	3616763.37	22.57	740119.11	20.46	700053.08	19.36	-14.23	652024.14	18.03	-11.90
14849	41565.45	158443.74	26.23	50206.11	31.69	47535.90	30.00	14.36	46628.81	29.43	-7.13
16079	687882.94	3289165.80	20.91	614550.63	18.68	579568.49	17.62	-15.75	530068.53	16.12	-13.75
13342	322310.34	2551665.46	12.63	355112.25	13.92	335043.85	13.13	3.95	301057.51	11.80	-15.22
18267	301927.78	3875293.99	7.79	242935.41	6.27	193594.78	5.00	-35.88	110279.80	2.85	-54.61
13703	646372.53	3265911.01	19.79	600413.05	18.38	401261.30	12.29	-37.92	350248.66	10.72	-41.67
15350	211709.96	1031234.49	20.53	207869.85	20.16	173288.94	16.80	-18.15	159226.23	15.44	-23.40
15951	501484.68	3118193.24	16.08	508799.51	16.32	363559.06	11.66	-27.50	313069.61	10.04	-38.47
14596	186896.11	1231545.27	15.18	171941.44	13.96	134361.45	10.91	-28.11	110412.39	8.97	-35.78
13340	142645.73	1023737.56	13.93	135757.46	13.26	65709.31	6.42	-53.94	42740.65	4.17	-68.52
12831	70616.82	414513.95	17.04	68797.43	16.60	39344.03	9.49	-44.29	34551.03	8.34	-49.78
14842	301955.52	1614386.70	18.70	279233.29	17.30	246487.63	15.27	-18.37	206692.03	12.80	-25.98

Appendix E. SWA-derived canopy-cover estimates for TEU polygons in the NO Bar project area

	2000					2008					
	30 threshold			70threshold		30threshold			70threshold		
Polygon ID	Crown Area	Polygon Area	Cover%	Crown Area	Cover%	Crown Area	Cover%	Change	Crown Area	Cover%	Change
12708	181951.09	1086952.53	16.74	159186.92	14.65	149878.61	13.79	-17.63	138185.62	12.71	-13.19
13209	23229.97	362718.71	6.40	11198.83	3.09	14501.09	4.00	-37.58	11396.15	3.14	1.76
13312	15522.97	105552.67	14.71	8828.70	8.36	10610.89	10.05	-31.64	7606.17	7.21	-13.85
13579	25902.83	369558.06	7.01	22992.65	6.22	20981.33	5.68	-19.00	19579.15	5.30	-14.85
13700	48810.60	205817.34	23.72	47670.93	23.16	47404.30	23.03	-2.88	46014.16	22.36	-3.48
13702	81764.27	664680.12	12.30	76334.27	11.48	74190.48	11.16	-9.26	63140.00	9.50	-17.28
13704	23523.26	211425.09	11.13	21882.85	10.35	18275.60	8.64	-22.31	15679.16	7.42	-28.35
14602	27000.39	306659.36	8.80	16744.43	5.46	24465.55	7.98	-9.39	9208.93	3.00	-45.00
14604	22692.52	298322.27	7.61	15098.85	5.06	26829.41	8.99	18.23	9486.74	3.18	-37.17
15143	274770.14	1950644.57	14.09	259028.21	13.28	242079.00	12.41	-11.90	229789.91	11.78	-11.29
15352	85988.19	1019634.71	8.43	91209.96	8.95	79854.91	7.83	-7.13	75147.36	7.37	-17.61
14844	49029.35	1357013.89	3.61	30516.65	2.25	37572.98	2.77	-23.37	22514.02	1.66	-26.22
14600	48207.51	674967.62	7.14	47035.15	6.97	38783.64	5.75	-19.55	36732.36	5.44	-21.90
15141	39906.30	445878.37	8.95	37891.18	8.50	35684.30	8.00	-10.58	33548.68	7.52	-11.46
14893	38119.29	320750.70	11.88	21903.14	6.83	27382.77	8.54	-28.17	22667.78	7.07	3.49
17491	93888.29	409673.28	22.92	88628.88	21.63	69596.58	16.99	-25.87	49644.56	12.12	-43.99
14591	122608.35	656919.25	18.66	128369.03	19.54	124669.33	18.98	1.68	115100.14	17.52	-10.34
14592	728393.35	2074497.02	35.11	719588.44	34.69	643219.30	31.01	-11.69	620509.27	29.91	-13.77
14594	114652.43	1715170.77	6.68	107651.32	6.28	100476.58	5.86	-12.36	84434.88	4.92	-21.57
14598	145773.09	465984.51	31.28	142934.85	30.67	137820.47	29.58	-5.46	134209.94	28.80	-6.10
15115	146996.04	888614.15	16.54	142348.32	16.02	115353.26	12.98	-21.53	107434.57	12.09	-24.53
15118	61979.13	363508.57	17.05	56211.86	15.46	51809.47	14.25	-16.41	46085.88	12.68	-18.01
15145	82390.57	235923.47	34.92	81136.85	34.39	83898.53	35.56	1.83	82437.26	34.94	1.60
16095	67999.65	202956.07	33.50	67604.90	33.31	59688.76	29.41	-12.22	58386.93	28.77	-13.64
16098	27779.97	382678.54	7.26	25679.57	6.71	16952.41	4.43	-38.98	8752.84	2.29	-65.92
15351	86761.33	426671.61	20.33	80097.19	18.77	64464.74	15.11	-25.70	46511.57	10.90	-41.93
15412	270669.60	1469930.38	18.41	215719.32	14.68	228733.68	15.56	-15.49	203939.05	13.87	-5.46
16845	196927.08	560966.29	35.10	193596.03	34.51	165519.34	29.51	-15.95	155133.67	27.65	-19.87
16847	6847.74	72115.97	9.50	6094.47	8.45	5003.27	6.94	-26.94	3708.91	5.14	-39.14
16097	147826.00	1268583.58	11.65	135261.86	10.66	113346.47	8.93	-23.32	89264.27	7.04	-34.01
15122	31869.55	183623.25	17.36	24181.44	13.17	25225.49	13.74	-20.85	22778.51	12.41	-5.80
15123	424406.53	3532144.71	12.02	390436.07	11.05	329611.21	9.33	-22.34	261947.90	7.42	-32.91
16094	76391.97	1007383.07	7.58	72765.46	7.22	60361.39	5.99	-20.98	52536.82	5.22	-27.80
13296	949983.40	4911435.11	19.34	699487.16	14.24	871570.49	17.75	-8.25	786575.66	16.02	12.45
17203	17711.01	196989.83	8.99	15336.54	7.79	16003.83	8.12	-9.64	13232.09	6.72	-13.72
17850	109284.66	832578.20	13.13	102484.13	12.31	94162.95	11.31	-13.84	83122.57	9.98	-18.89
18004	48127.77	402938.57	11.94	44768.21	11.11	45202.92	11.22	-6.08	39597.57	9.83	-11.55
14875	130838.95	338755.23	38.62	130394.85	38.49	128813.28	38.03	-1.55	128076.79	37.81	-1.78

Appendix F. Aerial photography documentation describing 2000 geometry and other parameters.

USGS Report No. OSL/2625

United States Department of the Interior

U.S. GEOLOGICAL SURVEY
Reston, Virginia 20192

REPORT OF CALIBRATION
of Aerial Mapping Camera

February 25, 2000

Camera type:	Wild RC30*	Camera serial no.:	5281
Lens type:	Wild Normal Aviogon II	Lens serial no.:	NAg II 7109
Nominal focal length:	210 mm	Maximum aperture:	f/4
		Test aperture:	f/4.6**

Submitted by: North West Geomatics Canada Inc.
Calgary, Alberta, Canada

Reference: North West Geomatics Canada Inc., purchase order No. 600158, dated February 24, 2000.

These measurements were made on Kodak Micro-flat glass plates, 0.25 inch thick, with spectroscopic emulsion type 157-01 Panchromatic, developed in D-19 at 68° F for 3 minutes with continuous agitation. These photographic plates were exposed on a multicollimator camera calibrator using a white light source rated at approximately 5200K.

I. Calibrated Focal Length: 213.956 mm

This measurement is considered accurate within 0.005 mm

II. Radial Distortion

Field angle	$\bar{D}_c$	D_c for azimuth angle			
		0° A-C	90° A-D	180° B-D	270° B-C
degrees	um	um	um	um	um
7.5	6	5	6	6	7
15	1	1	2	2	0
22.7	-4	-5	-4	-5	-3
30	2	2	2	2	2

The radial distortion is measured for each of four radii of the focal plane separated by 90° in azimuth. To minimize plotting error due to distortion, a full least-squares solution is used to determine the calibrated focal length. $\bar{D}_c$ is the average distortion for a given field angle. Values of distortion D_c based on the calibrated focal length referred to the calibrated principal point (point of symmetry) are listed for azimuths 0°, 90°, 180° and 270°. The radial distortion is given in micrometers and indicates the radial displacement away from the center of the field. These measurements are considered accurate within 5 um.

* Camera equipped with forward motion compensation
** Limitation imposed by collimator aperture

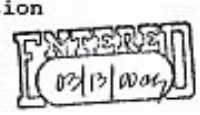

(1 of 3)

Appendix G. Aerial photography documentation describing 2008 geometry and other parameters.

USGS Report No. OSL/3439

United States Department of the Interior

U.S. GEOLOGICAL SURVEY
Reston, Virginia 20192

REPORT OF CALIBRATION
of Aerial Mapping Camera

February 06, 2009

Camera type:	Zeiss RMK A 21/23	**Camera serial no.:**	20209
Lens type:	Zeiss Toparon	**Lens serial no.:**	98310
Nominal focal Length:	210 mm	**Maximum aperture:**	f/5.6
		Test aperture:	f/5.6

Submitted by: Valley Air Photos
Caldwell, Idaho

Reference:

These measurements were made on Agfa glass plates, 0.19 inch thick, with spectroscopic emulsion type APX Panchromatic, developed in D-19 at 68° F for 3 minutes with continuous agitation. These photographic plates were exposed on a multicollimator camera calibrator using a white light source rated at approximately 5200K.

I. Calibrated Focal Length: 208.205 mm

This measurement is considered accurate within 0.005 mm

II. Radial Distortion:

Field angle	$\overline{D}_C$	D_C for azimuth angle			
		0° A-C	90° A-D	180° B-D	270° B-C
degrees	µm	µm	µm	µm	µm
7.5	-5	-3	-8	-7	-5
15	-4	-5	-2	-6	-5
22.7	-2	-4	-1	-4	1
30	5	3	6	4	6

The radial distortion is measured for each of four radii of the focal plane separated by 90° in azimuth. To minimize plotting error due to distortion, a full least-squares solution is used to determine the calibrated focal length. $\overline{D}_C$ is the average distortion for a given field angle. Values of distortion D_C based on the calibrated focal length referred to the calibrated principal point (point of symmetry) are listed for azimuths 0°, 90°, 180°, and 270°. The radial distortion is given in micrometers and indicates the radial displacement away from the center of the field. These measurements are considered accurate within 5µm.

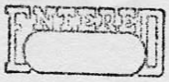

Page 1 of 3

References

Apache-Sitgreaves NF. 2011. Apache-Sitgreaves NF Website. <<http://www.fs.usda.gov/apache>> Accessed April 15, 2011.

Archer, S., D. S. Schimel, and E. A. Holland. 1995. *Mechanisms of shrubland expansion: Land use, climate or CO2?*. Climate Change **29**: 91-99.

Baker, W. L. 2009. *Fire ecology in Rocky Mountain landscapes.* Island Press, Washington. 1-605.

Baker, W. L., and D. J. Shinneman. 2004. *Fire and restoration of pinon-juniper woodlands in the western United States: a review*. Forest Ecology and Management **189**: 1-21.

Bradshaw, G.A., and T.A. Spies. 1992. *Characterizing canopy gap structure in forests using wavelet analysis*. Journal of Ecology **80**:205-215.

Burkhardt, J. W., and E. W. Tisdale. 1976. *Causes of juniper invasion in southwestern Idaho*. Ecology **57**(3): 472-484.

Chui, C. K. 1992. *An Introduction to Wavelets*. Academic Press, Inc. Boston, MA. 1-266.

Clark, J. T., M. V. Finco, R.Warbington, and B. Schwind. 2004. *Digital Mylar: A tool to attribute vegetation polygon features over high resolution imagery*. Proceedings: Remote Sensing for Field Users, Tenth Forest Service Remote Sensing Applications Conference. Salt Lake City, Utah, April 5 – 9, 2004. 1-7.

Clifton Ranger District. 2008. *Environmental assessment for Sunset restoration project*. Clifton Ranger District, Apache-Sitgreaves National Forest , US Forest Service: 1-54.

Covington, W.W. and M. M. Moore. 1994. *Changes in multiresource conditions in ponderosa pine forests since Euro-American settlement.* Journal of Forestry **92**(1): 39-47.

Dale, M. R. T. and M. Mah. 1998. *The use of wavelets for spatial pattern analysis in ecology*. Journal of Vegetation Science **9**: 805-814.

Daubechies, Ingrid. 1992. *Ten Lectures on Wavelets*. Society for Industrial and Applied Mathematics. Philadelphia, PA. 1-357.

Dwyer, D. D., and R. D. Pieper. 1967. *Fire effects on blue grama-pinyon-juniper rangeland in New Mexico*. Journal of Range Management **20**: 359-362.

ERDAS. 2008. ERDAS Imagine® and LPS® 9.3.1. ERDAS, Inc.

ESRI. 2006. ArcGIS® 9.2. ESRI, Inc.

Falkowski, M. J., A. M. S. Smith, A. T. Hudak, P. E. Gessler, L. A. Vierling, and N. L. Crookston. 2006. *Automated estimation of individual conifer tree height and crown diameter via two-dimensional spatial wavelet analysis of lidar data*. Canadian Journal of Remote Sensing **32**(2):153-161.

Ganey, J. L., and M. A. Benoit. 2002. *Using terrestrial ecosystem survey data to identify potential habitat for the Mexican spotted owl on national forest land: A pilot study*. US Forest Service, Rocky Mountain Research Station. General Technical Report RMRS-GTR-86: 1-30.

Garrity, S. R., L. A. Vierling, A. M. S. Smith, M. J. Falkowski, and D. B. Hann. 2008. *Automatic detection of shrub location, crown area, and cover using spatial wavelet analysis and aerial photography*. Canadian Journal of Remote Sensing **34**(2):376-384.

Goslee, S. C., K. M. Havstad, D. P. C. Peters, A. Rango, and W. H. Schlesinger. 2003. *High-resolution images reveal rate and pattern of shrub encroachment over six decades in New Mexico, U.S.A.* Journal of Arid Environments **54**: 755-767.

Hamilton, R., and K. Megown. 2005. *Monitoring and quantifying weed cover using a dot-grid sampling technique*. US Forest Service, Remote Sensing Applications Center: 1-9.

Jacobs, B. F. 2008. *Southwestern U.S. juniper savanna and pinon-juniper woodland communities: Ecological history and natural ranger of variability*. US Forest Service, Rocky Mountain Research Station. RMRS-P-51. 11-19.

Jameson, D. A. 1962. *Effects of burning on a galleta-black grama range invaded by juniper*. Ecology **43**(4): 760-763.

Jensen, J. R. 1996. *Introductory Digital Image Processing*. Prentice Hall. Upper Saddle River, NJ. 1-318.

Johnsen, T. N. 1962. *One-seed juniper invasion of northern Arizona grasslands*. Ecological Monographs **32**(3): 187-207.

Kaibab NF. 2011. Kaibab NF Website. << http://www.fs.usda.gov/kaibab >> Accessed April 15, 2011.

Laing, L., N. Ambos, T. Suirge, C. McDonald, C. Nelson, and W. Robbie. 1987. *Terrestrial ecosystem survey of the Apache-Sitgreaves National Forests*. Southwestern Region – US Forest Service.

Lever, R. 2008. *Prescribed Fire Specialist Report*. US Forest Service, Apache-Sitgreaves National Forest Clifton Ranger District: 1-42.

Lever, R., Personal Communication with author, November 3, 2010.

The Mathworks. 2009. Matlab® and Simulink®, Version 7.9 (R2009b).

Microsoft, Inc. 2003. Microsoft Office Excel® 2003.

Miller, R. F., and P. E. Wigand. 1994. *Holocene changes in semi-arid pinyon-juniper woodlands*. BioScience **44**(7): 465-474.

Romme, W. H., C. D. Allen, J. D. Bailey, W. L. Baker, B. T. Bestelmeyer, P. M. Brown, K. S. Eisenhart, L. Floyd-Hanna, D. W. Huffman, B. F. Jacobs, R. F. Miller, E. H. Muldavin, T. W. Swetnam, and R. J. Tausch, P. J. Weisberg. 2008. *Historical and modern disturbance regimes, stand structures, and landscape dynamics in pinon-juniper vegetation of the Western U.S.* Colorado Forest Institute, Colorado State University, Fort Collins, CO. 1-37.

Sankey, T. T., and M.J. Germino. 2008. *Assessment of juniper encroachment with the use of satellite imagery and geospatial data*. Rangeland Ecology & Management **61**(4): 412-418.

Slezak, E., A. Bijaoui, and G. Mars. 1990. *Identification of structures from galaxy counts – use of the wavelet transform.* Astronomy and Astrophysics **227**(2): 301-306.

SPSS, Inc., an IBM Company. 2010. SPSS Statistics 19.

Strand, E. K., A. M. S. Smith, S. C. Bunting, L. A. Vierling, D. B. Hann, and P. E. Gessler. 2006. *Wavelet estimation of plant spatial patterns in multitemporal aerial photography*. International Journal of Remote Sensing **27**(10): 2049-2054.

Strand, E. K. 2007. *Landscape dynamics in aspen and western juniper woodlands on the Owyhee Plateau, Idaho: A dissertation*. University of Idaho. 1-191.

Strand, E. K., L. A. Vierling, A. M. S. Smith, and S. C. Bunting. 2008. *Net changes in aboveground woody carbon stock in western juniper woodlands, 1946-1998.* Journal of Geophysical Research **113**: 1-13.

Tirmenstein, D. 1999. *Juniperus deppeana*. Fire Effects Information System Website. US Forest Service, Rocky Mountain Research Station, Fire Sciences Laboratory. <<http://www.fs.fed.us/database/feis/jundep/>> Accessed May 2, 2011.

Toney, C. and M. C. Reeves. 2009. *Equations to convert compacted crown ratio to uncompacted crown ration for trees in the Interior West*. Western Journal of Applied Forestry **24**(2): 76-82.

US Forest Service. 1990. US Forest Service Directive 2500. US Forest Service Directives Website. <<http://www.fs.fed.us/im/directives>>

US Geological Survey. 2011. Seamless Data Warehouse. << http://seamless.usgs.gov>> Accessed June 2, 2011.

West, N. E., and N. Van Pelt. 1987. *Successional patterns in pinyon-juniper woodlands*. Pinyon-juniper woodlands. Reno, NV, US Forest Service, Intermountain Research Station. 1-9.